

A 1.4-GHz Arecibo Survey for Pulsars in Globular Clusters

J. W. T. Hessels^{1,*}, S. M. Ransom², I. H. Stairs³, V. M. Kaspi¹, and P. C. C. Freire⁴

¹*Department of Physics, McGill University, Montreal, QC H3A 2T8, Canada;
hessels@physics.mcgill.ca*

²*National Radio Astronomy Observatory, 520 Edgemont Road, Charlottesville, VA 22903*

³*Department of Physics and Astronomy, University of British Columbia, 6224 Agricultural Road, Vancouver, BC V6T 1Z1, Canada*

⁴*NAIC, Arecibo Observatory, HC03, Box 53995, Arecibo, PR 00612*

**Current Address: Astronomical Institute “Anton Pannekoek”, University of Amsterdam, Kruislaan 403, 1098 SJ Amsterdam, The Netherlands*

ABSTRACT

We have surveyed all 22 known Galactic globular clusters observable with the Arecibo radio telescope and within 70 kpc of the Sun for radio pulsations at ~ 1.4 GHz. Data were taken with the Wideband Arecibo Pulsar Processor, which provided the large bandwidth and high time and frequency resolution needed to detect fast-spinning, faint pulsars. We have also employed advanced search techniques to maintain sensitivity to short orbital period binaries. These searches have discovered 11 new millisecond pulsars and 2 promising candidates in 5 clusters, almost doubling the population of pulsars in the Arecibo-visible globular clusters. Ten of these new pulsars are in binary systems, and 3 are eclipsing. This survey has discovered significantly more very fast-spinning pulsars ($P_{\text{spin}} \lesssim 4$ ms) and short orbital period systems ($P_{\text{orb}} \lesssim 6$ hr) than previous surveys of the same clusters. We discuss some properties of these systems, as well as some characteristics of the globular cluster pulsar population in general, particularly its luminosity distribution.

Subject headings: globular clusters: general — pulsars: general — binaries: general — radio continuum: stars — stars: neutron

1. Introduction

Currently, there are approximately 130 known pulsars in globular clusters (GCs)¹, of which about 60% are observed to be in binary systems.² Roughly two thirds of all the pulsars known in GCs have been discovered in only the last seven years by surveys (e.g. Possenti et al. 2003; Ransom et al. 2005a; Hessels et al. 2006) using low-temperature receivers ($T_{\text{rec}} \lesssim 35$ K) at central observing frequencies between $\nu_{\text{center}} = 1\text{--}2$ GHz, large bandwidth and high time and frequency-resolution backends (e.g. the Wideband Arecibo Pulsar Processor, Dowd, Sisk, & Hagen 2000, and the GBT Pulsar Spigot, Kaplan et al. 2005), advanced search techniques for binaries (e.g. Ransom, Eikenberry, & Middleditch 2002; Ransom, Cordes, & Eikenberry 2003; Chandler 2003), and copious amounts of processing time on dedicated computer clusters. Though a few non-recycled pulsars have been found in GCs (e.g. PSR B1718–19 in NGC 6342, Lyne et al. 1993), almost all known GC pulsars are MSPs. In fact, the 150 known GCs³ orbiting the Milky Way contain roughly three orders of magnitude more observed millisecond pulsars (MSPs) per unit mass than the Galactic plane, which contains approximately 60 known MSPs. GCs have proven to be the most fruitful place to look for MSPs partly because of the enormous stellar densities in their cores, which exceed those in the Galactic plane by up to six orders of magnitude. These conditions promote many different formation processes that create binary systems in which a neutron star can be spun-up, or “recycled” (Alpar et al. 1982; Radhakrishnan & Srinivasan 1982), through the accretion of matter from its companion star (see Camilo & Rasio 2005, the most up-to-date general overview of pulsars in GCs, for a review of the formation and evolutionary processes at work in the cores of GCs). Furthermore, the cores of GCs, where most of the MSPs reside, typically have radii less than an arcminute, small enough to be covered by a single telescope pointing. This affords the possibility of making single, deep multi-hour integrations for multiple faint MSPs in GCs, something that is not feasible in large area surveys of the field.

Some clusters contain many pulsars: Terzan 5 and 47 Tucanae harbor 33 and 22 known pulsars, respectively. Together, they contain 43% of the total known GC pulsar population (Camilo et al. 2000; Ransom et al. 2005a; Hessels et al. 2006). Finding numerous pulsars in a single cluster allows interesting studies of the cluster itself, in addition to the individual

¹A catalog of GC pulsars is maintained by P. C. C. Freire at <http://www.naic.edu/~pfreire/GCpsr.html>.

²Note however that, because binary pulsars are more difficult to detect than isolated pulsars, the observed binary fraction is a lower limit on the intrinsic binary fraction of the population.

³An online catalog of Milky Way GCs (Harris 1996) is maintained at <http://physun.physics.mcmaster.ca/Globular.html>.

pulsars contained therein. Such studies have included the detection of intra-cluster ionized gas (Freire et al. 2001), high mass-to-light ratios (D’Amico et al. 2002), and hints at the cluster’s dynamical history (Possenti et al. 2003). However, many clusters still contain no known pulsars at all, despite sensitive searches (Camilo & Rasio 2005). In some cases, this may simply be because pulsars are generally intrinsically weak objects and GCs are often distant (approximately 90% of the GCs orbiting the Milky Way are > 5 kpc from the Sun). Interstellar scattering, which broadens pulsations because of multi-path propagation, can also be a major obstacle, especially for MSPs in clusters at low Galactic latitudes. At low radio frequencies ($\lesssim 500$ MHz), scattering can completely wash out the signal of fast-spinning pulsars.

While GCs are clearly the most profitable targets for finding MSPs, these searches remain non-trivial. First, the requisite short sampling times ($< 100 \mu\text{s}$), high frequency resolution (< 0.5 MHz channels), long integrations (few hours), and large bandwidth (> 100 MHz) of these data can make data acquisition and storage formidable (data rates ~ 30 – 100 GB/hr). Recent surveys with relatively good sensitivity to binary pulsars have revealed that the majority of GC MSPs are in binaries. The pulsed signal from these binary pulsars is smeared in Fourier space by their orbital motion, and thus even a bright pulsar can go undetected if nothing is done to correct for this modulation over the course of a long observation. Advanced and computationally intensive techniques, which partially search orbital parameter space, are required to recover the majority of the lost signal. The extra effort required to find binaries is well justified however, as some of the most exotic pulsar binaries known have been found in GCs. For instance, PSR B1620–26 in the cluster M4 is in a hierarchical triple system with a white dwarf and a 1 – $3 M_{\text{Jup}}$ planet, the only planet known in a GC (Thorsett et al. 1999; Sigurdsson & Thorsett 2005); PSR J0514–4002 in NGC 1851, with an eccentricity of 0.89, is one of the most eccentric binary pulsars known (Freire et al. 2004); PSR B2127+11C in M15 is a rare double neutron star binary (Anderson et al. 1990); PSR J1748–2446ad in Terzan 5 is the fastest-spinning neutron star known (Hessels et al. 2006); and a few MSPs with possible main-sequence companions have been found (e.g. PSR J1740–5340, D’Amico et al. 2001, similar systems have not been found in the Galactic plane). Other exotic binaries, perhaps even an MSP-MSP binary or a MSP-black-hole binary, may have effective formation channels only in GCs (but see Sipior, Portegies Zwart, & Nelemans 2004).

Here we present searches for radio pulsations from 22 GCs, using Arecibo at central observing frequencies between 1.1–1.6 GHz. Roughly half of these clusters have been searched previously with Arecibo at 430 MHz (Anderson 1993; Wolszczan et al. 1989a,b). The highly successful Anderson (1993) survey found 11 of the 15 pulsars known in these clusters prior to the survey presented here. Our searches have uncovered 11 new MSPs and 2 promising

candidates in five clusters: M3, M5, M13, M71, and NGC 6749. Acceleration searches were crucial in finding all but 2 of these systems. Ten of the new pulsars are in binaries, 3 of which are eclipsing, with orbital periods of only a few hours. For comparison, no eclipsing systems were known in these clusters prior to our survey and only 5 of the 15 previously known pulsars were in binaries. Of the pulsars presented here, 9 out of 11 have $P_{\text{spin}} < 4$ ms. Only 2 of the 15 previously known pulsars in these clusters have $P_{\text{spin}} < 4$ ms, clearly demonstrating the improved sensitivity of this survey over past surveys to the fastest MSPs. In §2 we describe the targets, observational setup, and sensitivity of the survey. In §3 we outline the search procedure and analysis pipeline. In §4 we present the results of the survey. In the discussion of §5, we comment on the characteristics of the GC pulsar population in general, particularly its luminosity distribution. In §6, we conclude.

2. Observations

2.1. Targets

We observed every known Galactic GC visible from Arecibo⁴ and within 70 kpc of the Sun without any selection bias towards larger or denser clusters. The sample of 22 GCs is listed in Table 1, along with basic and derived cluster parameters (Harris 1996, unless otherwise indicated, all GC quantities used in this paper are from the 2003 February revision of the catalog). The numbers of known isolated and binary pulsars in each cluster are indicated, with figures in parentheses denoting the number of pulsars found by this survey. For clusters containing known pulsars, the average dispersion measure (DM) of the pulsars is indicated, as well as their spread in DM, which is in parentheses (for clusters where two or more pulsars have been found). For clusters with no known pulsar, the DM is also unknown; the values listed are derived from the Cordes & Lazio (2002) “NE2001” model for the distribution of free electrons in the Galaxy, using the Harris (1996) position and distance to the cluster.

2.2. Data Acquisition

Each cluster was observed at least twice for the full time it is visible with Arecibo (Table 1). The clusters were observed in one of two campaigns in the summers of 2001 and

⁴The declination range visible from Arecibo is approximately -1° to $+38^\circ$.

2002 using the Gregorian L-band Wide receiver⁵ ($T_{\text{rec}} \sim 35 \text{ K}$). Depending on the known or predicted DM of the cluster, the central observing frequency was either 1175 MHz ($\text{DM} \lesssim 100 \text{ pc cm}^{-3}$) or 1475 MHz ($\text{DM} \gtrsim 100 \text{ pc cm}^{-3}$). Our observations were made using the Wideband Arecibo Pulsar Processor (WAPP, see Dowd et al. 2000, for details), a digital auto-correlator with configurable sampling time (3 or 9-level samples) and number of lags. Generally, 3-level samples were autocorrelated with 256 lags, accumulated every $64\text{-}\mu\text{s}$, and summed in polarization before being written to the WAPP disk array as 16-bit numbers. For the few clusters with known or predicted DMs greater than 100 pc cm^{-3} , we used $128\text{-}\mu\text{s}$ sampling and 512 lags. These configurations were chosen in order to minimize dispersive pulse smearing and to take full advantage of the WAPP’s maximum sustainable data rate at the time of the observations (8 MB/s, or $\sim 30 \text{ GB/hr}$). Data were transferred to DLT magnetic tape for offline analysis and archiving. These observations resulted in about 4 TB of data on about 100 tapes.

At the time of our original cluster search observations, only one WAPP backend was available, providing 100 MHz of bandwidth. In more recent observations of M3, M5, M13, M71, and NGC 6749 (after December 2002), which were made as part of the timing observations of the new discoveries, we used three of the four available WAPP backends, each with 100 MHz of bandwidth centered at 1170, 1420 and 1520 MHz. The frequency gap between the lower and upper bands was to avoid persistent and intense radio frequency interference (RFI) in the frequency ranges 1220–1360 MHz and $> 1570 \text{ MHz}$. Using the PRESTO⁶ pulsar software suite, these data were partially dedispersed into a reduced number of subbands (generally 16 or 32 subbands) at the average DM of the cluster pulsars before further timing or search analysis. This process affords an order-of-magnitude reduction in data size (enabling transfer of these data over the internet from Puerto Rico to Canada), while still providing the possibility of creating dedispersed time series at a variety of DMs around the average DM of the cluster. These data were also searched for new pulsars, in the manner described in §3.

⁵For the initial searches, we used the original “L-Wide” receiver installed after the Arecibo upgrade in the 1990s. This is not the L-band Wide receiver currently available at Arecibo, which was installed in 2003 February and was used for most of our timing observations. Though having design differences, these two receivers have comparable sensitivity.

⁶See <http://www.cv.nrao.edu/~sransom/presto>.

2.3. Search Sensitivity

We can estimate the typical minimum flux density to which our searches were sensitive, as a function of the radiometer noise and observed pulsar duty cycle, using the equation

$$S_{\min} = \frac{\sigma \xi T_{\text{sys}}}{G \sqrt{n \Delta \nu T_{\text{obs}}}} \left(\frac{w_{\text{obs}}}{P_{\text{spin}} - w_{\text{obs}}} \right)^{1/2} \quad (1)$$

(following Dewey et al. 1985). The minimum signal-to-noise ratio (S/N) of a search candidate is indicated by σ , and is taken to be 10 here (although when candidate lists were short, due to a lack of RFI, we investigated candidates below this threshold). ξ is a factor that incorporates both losses due to the 3-level quantization of the signal and other systemic effects. Zero lag and van Vleck corrections (see Lorimer & Kramer 2004, and references therein) have been applied to our data. We use a value $\xi = 1.2$ to quantify the loss in sensitivity compared with infinite quantization. T_{sys} is the equivalent temperature of the observing system and sky (approximately 40 K toward our sources, which are predominantly at high Galactic latitudes). G is the telescope gain, which is a function of zenith angle, and is taken to have an average value of 10.5 K/Jy. For clusters that are only visible at zenith angles $\gtrsim 16^\circ$, the gain (and hence the sensitivity) is reduced by 5–15%. This is the case for the clusters which are closest to the declination limit of the Arecibo-visible sky: M2, M5, M13, Pal 5, Pal 15, NGC 6535, NGC 6749, and NGC 6760. n is the number of orthogonal polarizations that have been summed ($n = 2$ here). $\Delta \nu$ is the bandwidth of the backend, taken to be 100 MHz here. For clusters where subsequent timing observations were also performed (M3, M5, M13, M71, and NGC 6749), we were able to search a larger bandwidth (~ 250 MHz) by combining multiple WAPPs. T_{obs} is the integration time, which varies between clusters from 0.6–2.8 hr depending on the declination of the source, but is set to 2 hr for the purposes of these sensitivity calculations. w_{obs} is the observed pulse width, which is a function of the intrinsic pulse width w_{int} and other effects that smear the observed pulse profile (Equation 2). P_{spin} is the pulsar spin period.

When the DM of a cluster is not known, one must construct hundreds of trial time series at a wide range of DMs, each of which must be searched. Even for clusters with known DMs, the pulsars have a spread in DM, ΔDM , and several trial DMs must be searched in order to maintain maximum sensitivity. ΔDM increases roughly linearly with DM, and typically $\Delta \text{DM}/\text{DM}$ is a few percent (Freire et al. 2005).

The observed pulse width, w_{obs} in Equation 1, is always equal to or larger than the pulsar’s intrinsic pulse width w_{int} . Broadening is due to the finite time sampling of the data recorder, t_{samp} , dispersive smearing across individual frequency channels, t_{DM} , smearing due to the deviation of a pulsar’s true DM from the nominal DM of the time series used for

searching or folding, $t_{\Delta\text{DM}}$, and interstellar scattering, t_{scatt} . One can express the observed width as the sum in quadrature of these terms:

$$w_{\text{obs}}^2 = w_{\text{int}}^2 + t_{\text{samp}}^2 + t_{\text{DM}}^2 + t_{\Delta\text{DM}}^2 + t_{\text{scatt}}^2, \quad (2)$$

where the dispersive smearing (assuming the channel bandwidth $\Delta\nu_{\text{chan}} \ll \nu_{\text{center}}$) across an individual channel is given by

$$t_{\text{DM}} = 8.3 \left(\frac{\text{DM}}{\text{pc cm}^{-3}} \right) \left(\frac{\Delta\nu_{\text{chan}}}{\text{MHz}} \right) \left(\frac{\nu_{\text{center}}}{\text{GHz}} \right)^{-3} \mu\text{s}, \quad (3)$$

the smearing due to an incorrect DM in the time series is

$$t_{\Delta\text{DM}} = 4.1 \left[\left(\frac{\nu_{\text{low}}}{\text{GHz}} \right)^{-2} - \left(\frac{\nu_{\text{high}}}{\text{GHz}} \right)^{-2} \right] \left(\frac{\Delta\text{DM}}{\text{pc cm}^{-3}} \right) \text{ms}, \quad (4)$$

(where ν_{low} and ν_{high} are the low and high frequency edges of the bandwidth respectively), and the scattering (t_{scatt} is in ms) can be estimated by the empirical formula (Bhat et al. 2004)

$$\log_{10}(t_{\text{scatt}}) = -6.46 + 0.154 \log_{10}(\text{DM}) + 1.07 (\log_{10}(\text{DM}))^2 - 3.86 \log_{10} \left(\frac{\nu_{\text{center}}}{\text{GHz}} \right). \quad (5)$$

For these data at 1.4 GHz, $t_{\text{DM}} = 30\text{--}120 \mu\text{s}$ for DMs $25\text{--}200 \text{pc cm}^{-3}$ (using $\Delta\nu_{\text{chan}} = 100/256 \text{MHz}$ for $\text{DM} < 100 \text{pc cm}^{-3}$ and $\Delta\nu_{\text{chan}} = 100/512 \text{MHz}$ for $\text{DM} > 100 \text{pc cm}^{-3}$). In searches where the cluster DM was not known, we created dedispersed time series with DMs spaced by 1.0pc cm^{-3} . For clusters with known DMs, we typically used a spacing of 0.5pc cm^{-3} or finer. Hence, the maximum DM deviation between a pulsar’s true DM and that assumed in making the trial time series is 0.5pc cm^{-3} , resulting in a maximum smearing $t_{\Delta\text{DM}} = 150 \mu\text{s}$. We have estimated t_{scatt} using Equation 5 (Bhat et al. 2004), which predicts the scattering time based on the known (or predicted) DM and the observing frequency. t_{scatt} varies from source to source, but given the relatively high observing frequency of these data and the high Galactic latitudes of most of the sources observed here (most of which have relatively low known or predicted DMs), it does not significantly increase the smearing already present in the data.

Figure 1 shows the search sensitivity determined from Equations 1–5 as a function of

DM and period.⁷ We compare the sensitivity of our survey with that of the only other major survey of these clusters with Arecibo (Anderson 1993). As the Anderson (1993) survey was conducted at 430 MHz, we use a typical pulsar spectral index of -1.8 (Maron et al. 2000) as well as a flatter spectral index of -1.3 to scale that survey to 1400 MHz, so that the sensitivities of both surveys can be more directly compared.⁸ For low-DM pulsars with spin periods $\gtrsim 10$ ms and a standard spectral index ($\alpha = -1.8$), the Anderson (1993) survey had a similar sensitivity to ours. However, for pulsars spinning faster than this, especially those at high DMs and with relatively flat spectral indices, our survey provides a significant increase in sensitivity. For example, we were roughly 3–6 times more sensitive to a 2-ms pulsar at a DM of 100 pc cm^{-3} , assuming $-1.8 < \alpha < -1.3$.

Our searches are likely the deepest searches for GC pulsars yet undertaken. Though recent searches with Parkes (e.g. Camilo et al. 2000) and GBT (e.g. Ransom et al. 2005a) benefit from larger recordable bandwidth and longer possible source tracking times, Arecibo’s much larger gain still more than compensates for these (Table 2). Comparing raw gains, maximum tracking times, and recordable bandwidths, simple scaling using Equation 1 and a spectral index of -1.8 to compare different observing frequencies, shows that, with the currently available data-recorders, Arecibo has a raw sensitivity $4\times$ greater than Parkes and $2\times$ greater than the GBT for an isolated pulsar. For binary pulsars, where blind search sensitivity doesn’t improve as $T_{\text{obs}}^{1/2}$ (see §3.2 and 5.1.1.), and longer tracking times provide less benefit, Arecibo is more sensitive by an additional factor of roughly 2.

3. Analysis

3.1. Radio Frequency Interference Excision

Periodicities due to terrestrial radio frequency interference (RFI) can swamp search candidate lists. Ultimately this reduces a survey’s sensitivity by increasing the number of false positives. First, strong bursts of interference, principally from airport and military radars, were removed in the time domain by clipping samples found to be further than 6σ

⁷The degradation in sensitivity to binary pulsars caused by their orbital motion is *not* included in these estimates. We discuss our sensitivity to binary pulsars in §5.1.

⁸Maron et al. (2000) find a mean value for spectral index, α , of -1.8 ± 0.2 . It has been shown by a number of authors (e.g. Kramer et al. 1998; Toscano et al. 1998) that the mean spectral indices of MSPs and un-recycled pulsars are consistent with each other. Though radio pulsars, both MSPs and un-recycled, generally have steep, power-law spectra, the observed range of spectral indices in the pulsar population is large: $0 \gtrsim \alpha \gtrsim -4$.

from the mean in the $DM = 0 \text{ pc cm}^{-3}$ time series. Secondly, we created time-frequency masks and applied them to all data before searching. These masks remove certain channels during specific time intervals when either the maximum Fourier power, standard deviation, or mean of the data surpass statistically determined thresholds. This method was very useful at excising strong narrow-band and transient RFI from the data before searching and typically only $\lesssim 10\%$ of the data were masked. Lastly, we removed known “birdies” (weak but highly periodic broadband interference and bright known pulsars) from the power spectrum by setting the powers in these narrow frequency intervals to zero. We found that using these techniques and observing in the relatively RFI-clean frequency ranges of 1120–1220 MHz and 1370–1570 MHz kept the size of our candidate lists manageable, while minimizing the risk of rejecting potentially interesting candidates.

3.2. Search Techniques

In a standard Fourier-based search, which identifies pulsar harmonics above a certain threshold, binary pulsars are strongly selected against because of orbital modulation, which smears the signal power over many bins in frequency space. As the majority of MSPs in GCs are in binary systems, sometimes with orbital periods comparable to or shorter than the observation length, it is crucial to use more sophisticated techniques.

Our primary search method is a Fourier-based matched filtering technique (Ransom et al. 2002) which assumes that the pulsar’s orbit can be described by a constant acceleration (i.e. constant frequency derivative) over the course of the observation. This technique is a frequency-domain version of a previously used constant acceleration technique (Middleditch & Kristian 1984; Anderson et al. 1990; Camilo et al. 2000) in which the time series is quadratically stretched or compressed before it is Fourier transformed, in order to simulate different accelerations. The advantage of the Fourier-based technique used here is that it is computationally more efficient than the equivalent time-domain-based method, and provides even sampling of frequency derivative space. This method is typically most sensitive to binaries where the orbital period is $\gtrsim 10\times$ the integration time of the observation, although very bright pulsars with orbital periods much shorter than this can often be detected (Johnston & Kulkarni 1991). As our Arecibo observations were typically from 1–2.5 hr in length, for full tracks this search method is most sensitive to orbital periods $\gtrsim 10\text{--}25$ hr. Using the same technique, we also searched overlapping subsections of the data sets (which were typically about one third the total observation length), in order to be sensitive to larger accelerations and tighter binaries ($P_{\text{orb}} \gtrsim 3\text{--}10$ hr), as well as eclipsing systems.

To search for binaries with orbital periods a factor of ~ 2 or more shorter than the

observation time, we used a “phase modulation” search (Ransom et al. 2003; Jouteux et al. 2002). This method makes use of the change in phase of the pulsations from a binary pulsar and the “comb” pattern created by such a signal in the Fourier power spectrum. By taking Fast Fourier Transforms (FFTs) of short subsections of the power spectrum from the full observation, one can detect the sidebands, which are evenly spaced at the orbital period and centered on the true frequency of the pulsar. This method is appropriate for binary pulsars with orbital periods less than half the observation length, and increases in sensitivity as the ratio $T_{\text{obs}}/P_{\text{orb}}$ increases. Given the 1–2.5 hr integration times used in this survey, this technique was sensitive to an area of orbital parameter space in which no binary radio MSPs have yet been observed.

3.3. Data Analysis Pipeline

Here we summarize the data analysis pipeline applied to the observations of each cluster. The routines used in the pipeline are part of the PRESTO pulsar search and analysis package. First, we generated an RFI mask from the raw data (as described in §3.1). Applying this mask, a $DM = 0 \text{ pc cm}^{-3}$, topocentric time series was created and the corresponding power spectrum was examined by eye for periodic interference. We added the worst of the interference to the “birdie list” of frequency intervals to be subsequently removed from the Fourier transform. Again applying the RFI mask, we then dedispersed the data at a number of trial DMs using DM steps $\leq 1 \text{ pc cm}^{-3}$, clipping samples found to be greater than 6σ from the mean in the $DM = 0 \text{ pc cm}^{-3}$ time series. The time series were transformed to the solar-system barycenter during dedispersion, which allowed us to compare directly candidate periods from separate observations. This was very useful for distinguishing likely pulsar periodicities from the RFI background, which can vary greatly between observations. For clusters with known pulsars, we dedispersed at a range of trial DMs equal to at least 10% of the cluster’s average DM. For clusters with no known pulsars, we created time series at a range of DMs centered around the predicted DM of the cluster (Cordes & Lazio 2002), given its Galactic coordinates and distance in the Harris (1996) catalog. We assumed at least a 100% error in the predicted DM value when choosing a DM search range. For example, for a cluster with a predicted DM of 100 pc cm^{-3} , we searched dedispersed time series with $DM = 0\text{--}200 \text{ pc cm}^{-3}$. The dedispersion and subsequent analysis of the time series was conducted in parallel using multiple processors on a 52-node dual-processor Linux cluster called “The Borg”, located at McGill University and constructed by our group specifically for pulsar searches. Once the dedispersion was complete, the time series were Fourier-transformed. Our analysis did not restrict the number of samples in the time series to be a power of

two.⁹ We then set the frequency intervals of the birdie list to zero in the power spectra before searching the power spectra with both the phase-modulation and matched-filtering techniques described in §3.2.

As most pulsars have relatively short duty cycles, with spectral power divided between numerous harmonics, we summed harmonics in our matched-filter search to increase sensitivity to such signals. For each candidate signal, sums of 1, 2, 4, and 8 harmonics were tried and the optimum combination was determined. In these searches, we looked for signals where the highest of the harmonics used in summing drifted by up to $z_{\max} = 170$ bins in the Fourier domain. Higher order harmonics will drift by N_{harm} times more bins than the fundamental, where $N_{\text{harm}} = 1$ for the fundamental, $N_{\text{harm}} = 2$ for the second harmonic, etc. If, for example, 8 harmonics were summed in the identification of a particular candidate period, then the maximum number of bins the fundamental could drift by during the observation and still be detectable by our search would be $170/8$. Conversely, for signals where the fundamental drifted by more than $170/2$ bins during the observation, we were sensitive to at most one harmonic. The maximum number of bins a signal is allowed to drift corresponds to a maximum line-of-sight acceleration of $a_{\max} = z_{\max} c P_{\text{spin}} T_{\text{obs}}^{-2} N_{\text{harm}}^{-1} \simeq 4 P_{\text{spin,ms}} T_{\text{obs,h}}^{-2} N_{\text{harm}}^{-1} \text{ m s}^{-2}$, where $P_{\text{spin,ms}}$ and $T_{\text{obs,h}}$ are the spin period in milliseconds and the observation time in hours and N_{harm} is the highest order harmonic used in summing. Overlapping subsections of the observation, corresponding to about a third of the total observation length, were also searched using the matched-filtering technique and $z_{\max} = 170$ bins, in order to look for more highly accelerated pulsars.

The resulting candidate lists from the matched-filtering search were generally short enough that they could easily be examined by eye, although we also parsed candidate lists with a script that automatically folded candidates above an equivalent gaussian significance threshold of 7. Interesting candidates were folded using the estimated DM, period, and period derivative from the search and these parameters were optimized by the folding software to maximize the S/N ratio of the folded profile. The output plot from such a fold was used to determine whether a given candidate warranted further attention (see sample discovery plot and description in Figure 2). To identify potentially interesting candidates from the phase-modulation searches, we compared the search outputs from the different observing epochs of each cluster. The criteria for a promising phase-modulation candidate was a signal with a significance $> 10\sigma$ that did not peak in significance at $\text{DM} = 0 \text{ pc cm}^{-3}$, had an orbital period $> 600 \text{ s}$, and appeared, by virtue of a similar orbital period, in the candidate lists of at least two observing epochs.

⁹Some minimal padding was added to the data-sets however, so that the number of samples could be factored into primes where the maximum factor size was ≤ 13 .

4. Results

4.1. Redetections

Table 3 lists the 15 previously known pulsars in our survey clusters. The majority of these pulsars were easily detected by our search pipeline (Table 3). In fact, because many of these sources are relatively bright, masking these periodicities and their many significant harmonics was an important factor in reducing the length of candidate lists. The only previously known pulsars not detected in our searches are M15F, G, and H.¹⁰ Although these are all isolated pulsars, and are well within the $\sim 1.5'$ half-power radius of the 1.4-GHz Arecibo main beam, our non-detections are not very surprising: these are the dimmest pulsars in M15, and were all found in searches of multiple, combined observing epochs (Anderson 1993). Assuming standard spectral indices ($\alpha = -1.8$), they have flux densities right at the limit of our search sensitivity.

4.2. New MSPs

We have discovered 11 MSPs and 2 promising candidates in 5 clusters. Three of the clusters with new pulsars (M3, M71, and NGC 6749) contained no known pulsars prior to our survey. All of the pulsars discovered in this survey were found using the matched-filtering acceleration search technique, and all but the newly-found isolated pulsar M13C (PSR J1641+3627C) and the long-orbital-period binary M3D (PSR J1342+2822D) required a non-zero trial frequency derivative (acceleration) in order to be detectable. Given the criteria outlined in §3.3, no interesting candidates were identified by the phase-modulation search. The spin periods of the new pulsars have a narrow range 2.4–5.4 ms. For comparison, the previously known pulsars in these clusters have spin periods in the range 3.5–111 ms, with only 2 pulsars having $P_{\text{spin}} < 4$ ms. All but one of the new pulsars is in a binary system, with orbital periods ranging from 2.1 hr up to 129 d. Although none of the previously known binaries in these GCs show eclipses, 3 of the new pulsars found here eclipse. The basic characteristics of these pulsars are summarized in Table 4. Integrated pulse profiles, which are often the sum of numerous observations, are shown in Figure 3.

We have conducted monthly timing observations of these discoveries over the course of approximately two years using Arecibo and multiple WAPP backends. In fact, M3D (PSR J1342+2822D), M5E (PSR J1518+0204E), and M13E (PSR J1641+3627E) were all

¹⁰Note however that M15F was easily detected in complementary searches we made using the WAPP at 327 MHz (see §4.2.2).

discovered in searches of timing data because of fortuitous scintillation. The timing results for the M5 and M71 pulsars will be presented by Stairs et al. (2008, in preparation) and the timing of the M13 pulsars will be presented by Ransom et al. (2008, in preparation).

4.2.1. M3 (NGC 5272)

We have found the first three, and likely four, pulsars known in M3. All of these pulsars were detected in observations in which interstellar scintillation increased their flux to a detectable level and they are not consistently detectable with Arecibo. They have DMs within 0.3 pc cm^{-3} of each other, with an average DM of 26.4 pc cm^{-3} . This compares very well with the 23 pc cm^{-3} DM predicted by the NE2001 model (Cordes & Lazio 2002). On these grounds alone, there is little doubt that these pulsars are members of M3. M3A (PSR J1342+2822A) is a 2.54-ms binary which has only been detected three times, on MJDs 52491, 52492 and 52770 (we list the number of detections of each new pulsar in Table 4). Due to this paucity of detections, we do not currently know the orbital parameters for this pulsar, although its orbital period is likely on the order of a day. We also cannot derive a precise position for this pulsar, though we note that, since the half-power radius of the Arecibo 1.4-GHz main beam is $\sim 1.5'$, it is likely no further than this from the cluster center. M3B (PSR J1342+2822B) is a 2.39-ms binary in a 34.0-hr orbit with a $0.2 M_{\odot}$ (minimum mass) companion, which, in analogy to other systems with similar orbital parameters, may be a low-mass helium white dwarf. It is the most consistently detectable pulsar in M3, and is visible at least faintly in roughly half of our observations. On some occasions M3B has shown very large increases in flux (up to a flux density at 1400 MHz $S_{1400} \sim 0.1 \text{ mJy}$), presumably due to diffractive scintillation. We have derived a phase-connected timing solution for M3B (Table 5) using the TEMPO pulsar timing package¹¹ and standard pulsar timing techniques. This solution places it $8.3''$ (0.25 core radii) from the center of the cluster. Using this projected position and the simple cluster model outlined in Freire et al. (2005), we can derive the maximum contribution to the observed period derivative from acceleration in the cluster’s gravitational potential. In this model, we find $|a_{\text{max}}/c|P_{\text{spin}} = 1.6 \times 10^{-20} \text{ s/s}$, which is comparable to M3B’s observed period derivative. From this we place an upper limit on M3B’s *intrinsic* period derivative and corresponding lower limits on its characteristic age and dipole magnetic field (Table 5).

M3D has a spin period of 5.44 ms and an orbital period $\sim 129 \text{ d}$. Though the detections of M3D are too sparse to derive a phase-connected timing solution for this pulsar, by inserting

¹¹<http://www.atnf.csiro.au/research/pulsar/tempo>

arbitrary phase jumps between observing epochs we have been able to derive accurate orbital parameters, and a reasonably precise position (Table 5). M3D’s orbital period is much longer than the typical orbital period of GC MSPs, most of which have $P_{\text{orb}} < 3$ d, and may suggest a non-standard evolutionary history for the system. PSR B1310+18 in M53 ($P_{\text{orb}} \sim 256$ d, Kulkarni et al. 1991), PSR B1620–26 in M4 ($P_{\text{orb}} \sim 191$ d, Lyne et al. 1988), and PSR J1748–2446E in Terzan 5 ($P_{\text{orb}} \sim 60$ d, Ransom et al. 2005a) are the only other GC MSPs known to have orbital periods longer than 50 d. Binaries with orbital periods $10 \lesssim P_{\text{orb}} \lesssim 1000$ d may be efficiently formed by exchange interactions involving an isolated neutron star and “hard” primordial binaries (Hut et al. 1992; Sigurdsson & Phinney 1993). Camilo & Rasio (2005) point out that pulsars with long orbital periods (> 100 d) tend to reside in low-density clusters, i.e. $\rho_o < 4 \log_{10} L_{\odot}/\text{pc}^3$. As M3 has a central density $\rho_o = 3.51 \log_{10} L_{\odot}/\text{pc}^3$, M3D follows this trend. M3D also has a significant eccentricity, $e = 0.075$. This is significantly larger than expected from a single-stage stable-mass transfer episode from a red-giant (Phinney 1992), further pointing to an unusual evolution for this system.

We also have one very good candidate (denoted M3C in Table 4 because it was found before M3D and has been presented as such in previous references, e.g. Ransom et al. (2005c)) with a spin period of 2.17 ms that has been seen only once (presumably due to scintillation) with a S/N of ~ 6 during a ~ 3000 -s portion of an observation with the Green Bank Telescope (GBT), but never in any of our Arecibo data. During this single detection, the candidate showed a period drift of $1.82(3) \times 10^{-11}$ s/s, corresponding to a line-of-sight acceleration $a_l = 2.5 \text{ m/s}^{-2}$, indicating that, if it is real, this pulsar is in a binary system. These GBT data were taken with the Berkeley-Caltech Pulsar Machine (BCPM) as part of a parallel survey by our group for pulsars in GCs visible with the GBT (see Ransom et al. 2004, 2005c, for more details on these survey observations).

A deep radio synthesis image of M3 made at 1.4 GHz with the VLA (Kulkarni et al. 1990) revealed a $S_{1400} \sim 180 \mu\text{Jy}$ source $7.4''$ from the optical center of the cluster. This source does not coincide with the positions of M3B or M3D. In principle, the Kulkarni et al. (1990) radio source could be associated with M3A, M3C, or another unknown pulsar in the cluster. However, it seems too bright to be M3A or M3C, and unless it is particularly fast-spinning ($P_{\text{spin}} \lesssim 1$ ms) or highly accelerated by a companion star, its flux density should have made it easily detectable in our searches. It is of course also possible that the source is not associated with M3. Three 10-ks observations of the cluster with *Chandra* ACIS-S taken by Grindlay et al. (ObsIDs 4542, 4543, and 4544) reveal no obvious X-ray counterpart to the Kulkarni et al. (1990) radio source. There are however two obvious point sources within the half-mass radius of the cluster. One of these sources is coincident with the supersoft X-ray source 1E 1339.8+2837 (Dotani, Asai, & Greiner 1999). The other is not coincident

with the positions of either M3B or M3D.

4.2.2. *M5 (NGC 5904)*

In M5, we have found three new pulsars in addition to the isolated 5.55-ms pulsar M5A (PSR B1516+02A) and the binary 7.95-ms pulsar M5B (PSR B1516+02B) found by Wolszczan et al. (1989a), bringing the total population of this cluster to five. M5C (PSR J1518+0204C), with a spin period of 2.48 ms, is in a 2.1-hr orbit with a $0.04 M_{\odot}$ (minimum mass) companion. It shows regular eclipses for $\sim 15\%$ of its orbit as well as eclipse delays at eclipse ingress and egress, which can be up to ~ 0.2 ms and are presumably due to dispersive delays as the pulsar passes through the ionized wind of its companion. M5C is part of the growing class (Freire 2005) of ~ 10 eclipsing GC binaries with orbital periods of only a few hours and very low mass companions ($M_c \lesssim 0.1 M_{\odot}$). It is positionally coincident with a soft X-ray counterpart seen in a 45-ks *Chandra* ACIS-S observation of the cluster (Stairs et al. 2008, in preparation). M5D (PSR J1518+0204D), a binary 2.99-ms pulsar, was originally discovered in Arecibo data taken by our group at 327 MHz (see also Mott & Freire 2003), but it has also been seen at 1.4 GHz on numerous occasions because of scintillation. These 327-MHz data were obtained using the Gregorian 327-MHz receiver and the WAPP as part of a smaller set of search observations conducted at lower frequency on the clusters M3, M5, M13, and M15. M5D is in a 29.3 hr orbit with a $0.20 M_{\odot}$ (minimum mass) companion. M5E, a binary 3.18-ms pulsar, was discovered in a search of our regular timing observations of M5 and was visible because of scintillation. M5E has an orbital period of 26.3 hr and a $0.15 M_{\odot}$ (minimum mass) companion. It has a complex pulse profile and close to a 100% duty cycle (Figure 3).

4.2.3. *M13 (NGC 6205)*

In M13, we have found three new pulsars in addition to the isolated 10.4-ms pulsar M13A (PSR B1639+36A) and the binary 3.53-ms pulsar M13B (PSR B1639+36B) found by Kulkarni et al. (1991) and Anderson (1993), bringing the total population of this cluster to five. The pulsars in this cluster show $2\text{--}10\times$ changes in flux density because of scintillation on time scales shorter than an hour. M13C has a spin period of 3.72 ms and is the only isolated pulsar discovered in this survey. M13D (PSR J1641+3627D) is a 3.12-ms binary with a 14.2-hr orbital period and a $0.18 M_{\odot}$ (minimum mass) companion. M13E, a binary 2.49-ms pulsar, has been detected in only two observations, likely because of favorable scintillation. It is highly accelerated and appears to be eclipsed for part of each of these two observations.

We estimate that the orbital period is approximately 2.8 ± 0.2 hr, which is consistent with the interpretation that it is similar to M5C. The short orbital period and likely eclipses of this system make it difficult to blindly detect in a search. In analogy to other eclipsing MSPs, it is also likely that M13E will be visible as an X-ray source. Two roughly 30-ks *Chandra* observations of M13 were taken in March 2006, and may reveal an X-ray source coincident with this pulsar, or one of the others known in M13.

4.2.4. M71 (NGC 6838)

In M71, we have found M71A (PSR J1954+1847), the first and only pulsar known in this cluster. M71A’s DM of 117 pc cm^{-3} is reasonably close to the 86 pc cm^{-3} predicted by the NE2001 Galactic electron model (Cordes & Lazio 2002). It is also located ~ 0.6 core radii from the optical center of the cluster (see Stairs et al. 2008, in preparation), leaving little doubt it is associated with M71. M71A is a 4.89-ms pulsar in a 4.2-hr orbit with a $0.03 M_{\odot}$ (minimum mass) companion. It shows regular eclipses for $\sim 20\%$ of its orbit, though no eclipse delays are seen at ingress or egress. A discussion of its identification with an X-ray counterpart will be published elsewhere. The low density and relative proximity of M71 ($d = 4.0 \text{ kpc}$) make optical follow-up observations of M71A viable. The relatively high DM towards this cluster means diffractive scintillation has a small effect on the flux density of M71A. A stack search combining four contiguous days of data on this cluster revealed no new pulsars; searches combining more data sets will be undertaken.

4.2.5. NGC 6749 (Berkeley 42)

Lastly, we have found the first known pulsar in NGC 6749, as well as another promising pulsar candidate in this cluster. NGC 6749 has the lowest concentration ($c = \log_{10}(r_t/r_c)$) and the third lowest central luminosity density (tied with M13) of any GC with a known pulsar. NGC 6749A is a 3.19-ms binary pulsar with an orbital period of 19.5 hr and a $0.090 M_{\odot}$ (minimum mass) companion. Though there is no evidence for eclipses in the system, we cannot rule them out, as orbital coverage around superior conjunction is poor. The DM of NGC 6749A (PSR J1905+0154A) is 194 pc cm^{-3} , which is significantly lower than the 438 pc cm^{-3} DM predicted by the NE2001 model (Cordes & Lazio 2002). Due to the sparseness of measured arrival times at some epochs, we have only been able to derive a *partially* phase-connected timing solution for this pulsar (Table 5), which places the pulsar $0.51 \pm 0.38'$ (~ 0.7 core radii) from the center of the cluster. Thus, an association between

this pulsar and NGC 6749 is quite secure¹², and the DM discrepancy could easily be due to uncertainties in the NE2001 model, or perhaps an overestimation of the cluster’s distance.

NGC 6749B (PSR J1905+0154B) is a candidate 4.97-ms binary pulsar that has been seen only once, in data from MJD 52921. Although it is quite faint – the detection has a S/N of ~ 5 – the signal shows a clear peak in DM at roughly 192 pc cm^{-3} . The similarity in DM with NGC 6749A bolsters this candidate’s identification as a real pulsar and member of NGC 6749. In the one 5000-s observation where this candidate was seen, it showed a period drift of $-1.53(2) \times 10^{-11} \text{ s/s}$, corresponding to a line-of-sight acceleration $a_l = -0.9 \text{ m s}^{-2}$, and indicating that, if this is a real pulsar, it is in a binary system.

5. Discussion

5.1. Survey Limitations

In this section, we discuss the limitations of this survey due to a number of observational and analytical biases. Before we do, it also bears reminding the reader that the number of pulsars we can find is also limited in a more fundamental way by the clusters’ efficiency at creating them. From theoretical expectation and mounting observational evidence, it is becoming clear that cluster density has an important role to play in creating MSPs in a GC. Currently, no cluster with a central luminosity density of $\rho_o < 3 \log_{10} L_\odot/\text{pc}^3$ contains a known pulsar. Conversely, Terzan 5 and 47 Tuc have central densities of $\rho_o = 5.06$ and $4.81 \log_{10} L_\odot/\text{pc}^3$ respectively and have the largest known populations. We have surveyed all 22 GCs visible from Arecibo and within 70 kpc without any bias against observing low-density clusters. Unfortunately, from the point of view of wanting to find as many new pulsars as possible, these clusters are on average not very dense compared with clusters in the Galactic bulge, outside of Arecibo’s field of view. Of the 22 clusters in our survey, 8 have $\rho_o < 3 \log_{10} L_\odot/\text{pc}^3$ and still contain no known pulsar. This is not a great surprise. Of the remaining 14 clusters, which have densities in a range where one might expect to find pulsars, 8 have known pulsars. The absence of any known pulsar in the remaining 6 survey clusters with $\rho_o > 3 \log_{10} L_\odot/\text{pc}^3$ can be mostly explained by their large distances (see also §5.1.2).

¹²NGC 6749 sits in the Galactic plane at a latitude of -2.2° . Using the number of observed field MSPs in the Galactic plane to roughly estimate the angular density of observable MSPs, we use this number and the angular distance of NGC 6749A from the cluster center to estimate a chance association probability of $\sim 10^{-8}$.

5.1.1. Sensitivity to Fast and Binary Pulsars

The fastest-spinning pulsar known is PSR J1748–2446ad in Terzan 5, with a spin period of 1.396 ms (Hessels et al. 2006) and the shortest known orbital period of any binary MSP is 1.6 hr (PSR J0024–7204R in 47 Tucanae, Camilo et al. 2000). Here we discuss the sensitivity of this survey to very-fast-spinning pulsars ($P_{\text{spin}} \sim 0.5\text{--}3.0$ ms) and/or pulsars in very tight orbits ($P_{\text{orb}} \sim 0.5\text{--}6.0$ hr). The discovery of such systems is hampered by a number of selection effects (Johnston & Kulkarni 1991; Ransom et al. 2003), which bias the observed spin and orbital period distributions to longer periods. We discuss the extent to which the observed spin period distribution of the total population of MSPs has been affected by selection effects in §5.2.

We have characterized the sensitivity of this survey, as a function of period and DM, in §2.3 and compare it to the sensitivity of the Anderson (1993) survey (Figure 1). Though the survey’s sensitivity to slow pulsars ($P_{\text{spin}} \gtrsim 10$ ms in this case) is shown to be flat, there is undoubtedly some extra, unmodeled reduction in sensitivity to very slow ($P_{\text{spin}} \gtrsim 0.5$ s) pulsars because of RFI and red-noise. We note however that very few slow pulsars are known in the GC system and we do not a priori expect such systems in the clusters we have surveyed because they are generally found in higher-density clusters (Camilo & Rasio 2005).

For $\text{DM} = 30 \text{ pc cm}^{-3}$, our sensitivity to a 1-ms pulsar is degraded by a factor of roughly 1.5 compared with a 4-ms pulsar. This degradation in sensitivity is a strong function of DM and increases to a factor of ~ 2.5 at a DM of 200 pc cm^{-3} . Some of the MSPs we have discovered in this survey were just barely detectable by our processing (e.g. NGC 6749A and M3D). We can thus not rule out the existence of pulsars with $P_{\text{spin}} \lesssim 1.5$ ms in our survey data, if they have fluxes comparable to the dimmest sources we have discovered. However, a “reasonably bright” ($S_{1400} > 50 \mu\text{Jy}$), *isolated* 1-ms pulsar would very likely have been detected. We discuss the *luminosity* limits achieved for individual clusters, which depend largely on the cluster distance, in the next section. Even higher time and frequency resolution data are required to maintain as flat a sensitivity response as possible out to spin periods below ~ 1 ms. This should be a goal of future surveys and is feasible given the current state of computer technology.

The shortest spin period found in this survey was 2.4 ms (M3B). Furthermore, 5 of the 11 pulsars found here have spin periods between 2–3 ms, significantly lower than the median period of the observed population of GC MSPs, which is 4.7 ms (see Figure 4, left, for a spin period histogram of all known GC pulsars). For comparison, the fastest-spinning pulsar known in these clusters prior to this survey is M13B, with a spin period of 3.5 ms. This demonstrates the increased sensitivity of this survey to fast-spinning pulsars, compared with previous surveys, and suggests that the observed spin-period distribution of GC pulsars is

still artificially biased towards longer spin periods. This is unsurprising if one compares the sensitivity curves of this survey with those of Anderson (1993), as in Figure 1.

Our sensitivity to short orbital periods is difficult to quantify precisely. We compare the sensitivity of a coherent search of the data (i.e. one in which the orbital modulation of the pulsar signal can be completely corrected, and in which the sensitivity is proportional to $T_{\text{obs}}^{-1/2}$) to that of our acceleration search technique, using the simulations of Ransom et al. (2003), which were made using the same search technique and software. These simulations assume a pulsar spin period of 2 ms and a companion mass of $0.1 M_{\odot}$. We see that for a 2-hr binary period and a 0.5-hr observation duration that the sensitivity afforded by an acceleration search is roughly half that of the coherent sensitivity. A 0.5-hr observation duration is typical of the length used in our short subsection searches, and thus for all clusters we had good sensitivity to orbital periods down to a few hours. Specifically for the survey clusters with known pulsars (where the DM is thus also known), we searched a larger variety of short subsections of the total observation length, down to integration times as short as roughly 10 minutes. For these clusters, we were sensitive to even more compact systems and higher accelerations (assuming the pulsar’s flux is high enough to show up in such short integrations).

As explained in §3.3, in our matched-filter acceleration technique we looked for signals where the highest order harmonic used in summing drifted by up to $z_{\text{max}} = 170$ bins, corresponding to a maximum line-of-sight acceleration of $a_{\text{max}} \simeq 4P_{\text{spin,ms}}T_{\text{obs,h}}^{-2}N_{\text{harm}}^{-1} \text{ m s}^{-2}$. For comparison, we note that Camilo et al. (2000) were sensitive to a maximum acceleration of $< |30| \text{ m s}^{-2}$ in their searches of 47 Tucanae (where 0.3-h integration subsections were used) and that PSR B1744–24A in Terzan 5 has a maximum line-of-sight acceleration of 33 m s^{-2} (Lyne et al. 1990). For $P_{\text{spin}} = 2 \text{ ms}$ and $T_{\text{obs}} = 0.5 \text{ h}$, which is typical of the integration times used in our short-subsection searches, we reach a limiting acceleration of 32 m s^{-2} (note however that this limit applies only to the fundamental and not to sums including higher-order harmonics). For clusters where we searched numerous timing observations, $z_{\text{max}} = 500$ bins was sometimes used, providing an additional factor of three range in acceleration space. Such high accelerations are worth exploring in order to maintain sensitivity to not only the accelerated fundamental of a pulsar signal but also its harmonics, which are needed to detect faint pulsars. Though no new pulsars were found in these searches, we note that the pulsars M13E and M71A were only detected with 1 – 2 harmonics in our initial $z_{\text{max}} = 170$ searches and would have been more easily identified in a $z_{\text{max}} = 500$ search. Re-searching the data presented here with $z_{\text{max}} = 1000$ has the potential to discover compact binaries that were previously missed.

The most extreme orbital systems we found in this survey were M5C, M13E, and

M71A, with orbital periods between $\sim 2\text{--}4$ hr and minimum companion masses between $\sim 0.02\text{--}0.1 M_{\odot}$. As 10 of 11 pulsars found here are in binary systems, this survey did a good job of detecting the binaries that were missed by Anderson (1993) and other previous searches of these clusters.¹³ With the exception of the long orbital period binary M3D, all the binaries presented here required the acceleration search technique in order to be detected. The fact that we found only 1 isolated pulsar suggests that previous surveys already found the vast majority of the reasonably bright isolated pulsars in these clusters.

5.1.2. Sensitivity to the Weakest Pulsars

Of the 22 clusters we have searched for pulsations, 14 still contain no known pulsar, although all of these (with the exception of M2) are > 15 kpc from the Sun and/or have very high predicted DMs ($> 150 \text{ pc cm}^{-3}$). We have estimated the maximum luminosity of any undiscovered pulsars in the clusters we have searched, using the distance to the cluster, its DM (or predicted DM), and the sensitivity calculations of §2.3. These upper limits are given in Table 1, and apply most directly to isolated pulsars. For comparison, the weakest-known pulsars in Terzan 5 have 1400-MHz luminosities¹⁴ $L_{1400} \sim 2 \text{ mJy kpc}^2$, and the weakest in 47 Tucanae are $L_{1400} \sim 1 \text{ mJy kpc}^2$. Furthermore, there are indications that the *intrinsic* lower limit for the MSPs in 47 Tucanae is $L_{1400}^{\text{min}} \approx 0.4 \text{ mJy kpc}^2$ (McConnell et al. 2004). Because of their large distances, such weak pulsars are not excluded in any of the clusters we have searched here. For most of our clusters, the luminosity limits only exclude pulsars whose luminosity is comparable to the brightest MSPs known in the GC system ($L_{1400} \gtrsim 5 \text{ mJy kpc}^2$). Significantly more sensitive observing systems (using, for example, the Square Kilometer Array) will be required to fully probe the pulsar populations of these clusters down to the proposed low-luminosity cutoff.

5.1.3. Spatial Coverage

Here we investigate whether our single-pointing observations provided adequate spatial coverage to discover the bulk of the visible pulsars in our survey clusters. The vast majority

¹³However, we note that five of the eight pulsars found in M15 by Anderson (1993) are especially faint, isolated pulsars discovered in searches of multiple M15 data sets. M15D and E were found in incoherent stack searches of multiple observations, while M15F, G, and H were found in coherent multi-day transforms. These searches are *much* less sensitive to binary systems.

¹⁴This is a “pseudo” luminosity, defined as $L_{1400} \equiv S_{1400} d^2$.

of GC pulsars are found close to the centers of their clusters due to mass-segregation of the massive neutron stars. Of the GC pulsars with measured angular distance from their host cluster’s center, r , roughly 90% are at $r/r_c < 3$ (see e.g. Camilo & Rasio 2005), where r_c is the cluster’s core radius (these are listed for each of our survey clusters in Table 1). Pulsars further from their cluster center ($r/r_c \gtrsim 5$) are found predominantly in high-density ($\rho_o \gtrsim 4.5 \log_{10} L_\odot/\text{pc}^3$) clusters (Camilo & Rasio 2005). Only one of our clusters, M15, has such a high density, and thus we do not a priori expect that such sources exist in our other survey clusters.

The radius of the Arecibo beam at 1.4 GHz is roughly $1.5'$. Thus, for the 12 clusters we surveyed with $r_c < 0.5'$, almost all of the cluster’s pulsars should have fallen within our beam. Furthermore, the beam radius of the 430-MHz Anderson (1993) survey, which observed 11 of the same sources (see Table 1), was $5'$, and would likely have detected some sources further from the cluster centers, if they existed. For the 6 clusters we surveyed with $r_c < 1.0'$, the coverage was still very good, though perhaps 20% of the pulsar population fell outside the Arecibo beam. There remain 4 survey clusters whose r_c is comparable to the beam half-power radius or larger: NGC 5053 ($r_c = 1.98'$), NGC 5466 ($r_c = 1.64'$), Pal 5 ($r_c = 3.25'$), and Pal 15 ($r_c = 1.25'$). In these clusters, perhaps only half of the pulsar population fell within the Arecibo beam. In general however, we conclude that it is unlikely that a significant number of pulsars were missed in this survey because of spatial coverage.

5.2. MSP Spin Frequency Distribution

If one includes both the known MSPs in the field and those in GCs, the *observed* distribution of radio pulsar spin frequencies above 200 Hz roughly follows a power-law relationship with an index of -3 , i.e. $N_{\text{psr}} \propto \nu_{\text{spin}}^{-3}$ (Figure 4, right). We do not suggest that the underlying spin-frequency distribution is a power-law, or that a physical motivation for this choice exists, we merely use this functional form to quantify the sharp observed drop in the number of known pulsars as ν_{spin} increases. Considering the combined spin frequencies of MSPs in the field and in GCs is potentially problematic, as the frequency distributions of MSPs in the field and those in GCs could well be intrinsically different. Furthermore, the spin-frequency distribution between GC MSP populations may also vary (e.g. there is some indication that Terzan 5 has a wider range of spin frequencies than 47 Tucanae). Nonetheless, for the purposes of discussing the effect of observational bias on the observed spin frequency distribution, we will consider the MSP population as a whole.

There is no significant correlation currently observed between the radio luminosity of MSPs and their spin frequency. Because all other conceivable observational biases (e.g. scat-

tering, dispersive smearing, self-obscuration) *increase* the difficulty in detecting the fastest pulsars, the observed spin-frequency distribution above 200 Hz places a limit on the steepness of the intrinsic spin frequency distribution at these frequencies (i.e. if $N_{\text{psr}} \propto \nu_{\text{spin}}^{-\alpha}$, then $\alpha_{\text{true}} < \alpha_{\text{obs}}$). We now consider the observational biases that contribute to the observed spin-frequency distribution of MSPs. First, we see from Equation 1 that the minimum detectable flux density depends on spin frequency because pulse smearing due to scattering and DM has a greater relative effect for fast pulsars. This accounts for part of the slope in the observed spin-frequency distribution. Second, as there is no indication that orbital period is strongly correlated with spin frequency, it is unlikely that many of the fastest MSPs are being missed because they are preferentially in the most compact orbits. However, the number of bins through which a binary-modulated pulsar signal will drift in the Fourier domain is directly proportional to its spin frequency. In other words, for the same orbital period, it is more difficult to detect a 1-ms pulsar than a 5-ms pulsar in an acceleration search, because the 1-ms pulsar (and its harmonics) will drift by a factor of 5 times more Fourier bins. Harmonics that drift by many bins are more susceptible to non-linear frequency drift terms (reducing their detectability) and may drift beyond the maximum number of bins probed by the search (z_{max}). Thus, binary motion also accounts for part of the slope in the observed spin-frequency distribution, although this effect is difficult to quantify. Finally, because it is plausible that eclipse fraction increases with $\dot{E} = 4\pi^2 I \nu \dot{\nu} \propto B_{\text{surf}}^2 \nu^4$ (assuming that the pulsar spindown is dominated by magnetic dipole radiation), fast-spinning pulsars in binary systems may be preferentially obscured by the material their strong winds ablate from their companions (Tavani 1991; Hessels et al. 2006).

Given the multitude of observational biases against detecting the fastest-spinning radio pulsars, it is difficult to identify what portion of the observed spin-frequency distribution is intrinsic to the population. Perhaps the best way to investigate this problem is by performing Monte Carlo simulations of various trial underlying populations and then searching these until one converges on the observed population. Terzan 5 and 47 Tucanae present excellent samples on which to perform such simulations, although one would have to be careful in generalizing the results to MSPs in the field or in other GCs. If the distribution of radio pulsar spin frequencies is even approximately like that of the LMXBs, which is roughly consistent with being flat over the observed range of 270–619 Hz (Chakrabarty et al. 2003), then we have still only discovered a very small fraction of the fastest-spinning radio pulsars. Mapping the distribution at the fastest spin frequencies depends crucially on finding these pulsars.

5.3. Pulsar Luminosities

In Table 4, we list the 1.4-GHz flux densities of the pulsars discovered in this survey, as well as those of the previously known pulsars in these clusters.¹⁵ These were derived from the observed pulse profiles by integrating the pulse and scaling this flux using the off-pulse root mean square and the radiometer equation. For the mostly non-scintillating pulsars M71A and NGC 6749A, we estimate that the fractional uncertainty on their flux is roughly 30%. For the pulsars found in M3, M5, and M13, scintillation can have a strong effect on the observed flux of the pulsars as a function of time, making it more difficult to estimate the underlying intrinsic brightness of these sources. For these pulsars, we have used an approach similar to that used by Camilo et al. (2000): we fit the observed fluxes – using half the survey sensitivity limit as the flux in the case of non-detections – to an exponential distribution, whose median value we take as the intrinsic flux. This approach worked well for many of the scintillating pulsars in M3, M5, and M13, which were detected in the majority of our many ($\gtrsim 50$) timing observations of these clusters. For these pulsars, we estimate that the fractional uncertainty on their quoted flux density is 50%. The exceptions were M3A, M5E, and M13E, where the scarcity of detections made determining the intrinsic flux density more uncertain. The quoted flux densities of these sources have a higher fractional uncertainty of roughly 70%.

The luminosity distribution of MSPs, both in the field and in GCs, has been difficult to constrain precisely because of the relatively small number of known MSPs and the observational biases against finding faint, fast, and binary pulsars. Furthermore, individual estimates of pulsar luminosity can suffer from large systematic errors because the distance is incorrect. This is especially difficult in the field, where most distances are estimated from the DM, but is less of an issue for pulsars associated with GCs, whose distances are known comparatively precisely. In this section, we take advantage of the many new pulsar discoveries that have been recently made in GCs. We combine the luminosities of the pulsars currently known in M5, M13, M15, M28, NGC 6440, NGC 6441, 47 Tucanae, and Terzan 5 (see Table 6) and consider the resulting luminosity distribution of GC MSPs. These specific GCs were chosen because they contain at least 4 pulsars each. The clusters M3, M62, NGC 6624, and NGC 6752, which are the only other clusters with at least 4 known pulsars, were excluded from the analysis because reliable fluxes were not available for all the known pulsars in these clusters.

In Figure 5, we plot the 1.4-GHz cumulative luminosity distribution of 41 isolated (top

¹⁵We provide only upper limits, determined from the raw sensitivity of the survey, on the flux densities of the candidate pulsars M3C and NGC 6749B.

left), 41 binary (top right), and all 82 pulsars in our sample combined (bottom). In the majority of cases, specific spectral indices were not available, and luminosities were scaled to 1.4 GHz (where necessary) assuming a pulsar spectral index of $\alpha = -1.8$ (Maron et al. 2000). Unless otherwise indicated, the Harris (1996) catalog distance to the host GC was used to convert 1400-MHz flux density S_{1400} to pseudo luminosity $L_{1400} \equiv S_{1400}d^2$ (see Table 6). The M5 and M13 luminosities are from the observations made in this survey. The Terzan 5 luminosities come from Ransom et al. (2005a) and subsequent analysis of the more recently found pulsars in this cluster. We assumed a distance of 8.7 kpc to Terzan 5 (Cohn et al. 2002). The 47 Tucanae fluxes are from Camilo et al. (2000) and we use a distance of 4.5 kpc (Zoccali et al. 2001) to convert these to luminosities. The luminosities of pulsars in M28, NGC 6440, and NGC 6441 come from recent 1950-MHz discoveries and timing observations made by our group with the GBT (Ransom et al. 2005b; Bégin 2006, these discoveries are currently being prepared for publication as Bégin et al. and Freire et al.).

We fit $\log_{10}(N > L)$ versus $\log_{10}(L)$ to a line, using the square-root of $\log_{10}(N > L)$ as the uncertainties. These best-fit slopes are shown as solid lines in Figure 5. No corrections have been made for any observational bias (as has been done for field MSPs in Lyne et al. 1998; Cordes & Chernoff 1997). For all isolated and binary pulsars combined, the best-fit slope is -0.77 ± 0.03 . Below 1.5 mJy kpc² the observed distribution turns over, and thus we used a minimum luminosity cut-off of $L_{1400}^{\min} = 1.5 \text{ mJy kpc}^2$ for fitting purposes. Only the 70 pulsars in our sample above this luminosity limit were included in the fit. In combining luminosities from numerous clusters, we have assumed that the luminosity function does not vary significantly between clusters. We note that, when the same analysis is applied separately to the pulsar populations of the individual GCs in our sample, the slope is in each case consistent with that derived from all clusters in our sample combined (though the error on the slope is of course large for clusters with few known pulsars). This supports the assumption that the radio luminosity distribution of GC pulsars is universal. As 40% of the sample pulsars are in Terzan 5, it is important to ask how much the assumed distance to the cluster affects the combined luminosity distribution. We find that the distance to Terzan 5 can change by up to 30%¹⁶ without significantly altering the slope derived from all the different cluster pulsars combined. Furthermore, 56% of the pulsars in our sample are contained in either Terzan 5 or 47 Tuc. These two clusters thus have a large influence on the derived luminosity law, and it will be important to revisit these calculations when larger pulsar populations are known in other clusters as well.

There are clearly ripples in the combined distribution, suggesting unmodeled effects,

¹⁶This encompasses the range of published distances to Terzan 5, including the newest derived distance of $5.5 \pm 0.9 \text{ kpc}$ from Ortolani et al. (2007).

possibly due entirely to observational biases. When the population is separated into isolated and binary pulsars, it is clear that these effects come predominantly from the binary pulsars. This is perhaps unsurprising, as the observational biases inherent in detecting such systems are significantly higher than for the isolated pulsars. Considering only the 37 isolated pulsars in our sample above L_{1400}^{\min} , we find a much smoother distribution, with a best-fit slope -0.90 ± 0.07 . Conversely, the cumulative distribution of the 33 binaries above L_{1400}^{\min} is relatively poorly fit by a single slope of -0.63 ± 0.06 . We note that while the slope derived by fitting the isolated pulsars is relatively insensitive to the value of L_{1400}^{\min} (as long as it is not well below 1.5 mJy kpc^2), the slope derived from the binary pulsars varies significantly as L_{1400}^{\min} is changed.

Given the much lower bias against detecting isolated pulsars, we suggest that the slope derived from fitting only isolated pulsars is the most reliable. This distribution is somewhat flatter, though still barely consistent with the $d \log_{10}(N) = -d \log_{10}(L)$ relation found for non-recycled field pulsars and MSPs (consider for instance Lyne, Manchester, & Taylor 1985; Lyne, Manchester, Lorimer, Bailes, D’Amico, Tauris, Johnston, Bell, & Nicastro 1998; Cordes & Chernoff 1997). It is also roughly consistent with the recently derived luminosity law of Lorimer et al. (2006), who find $d \log_{10}(N) \sim -0.8 d \log_{10}(L)$ using a sample of 1008 normal (non-millisecond) pulsars. As the population of known GC MSPs continues to increase, we will be better able to constrain the luminosity distribution. However, until the next large advance in telescope collecting area, it will be hard to constrain the luminosity function of GC MSPs below 1 mJy kpc^2 , because of the relatively large distances to GCs and selection effects, which are worse for weak pulsars.

We note that 70% of our sample pulsars, those in M15, M28, NGC 6440, NGC 6441, and Terzan 5, can be characterized as not strongly scintillating (Table 6). Thus, as the majority of the pulsars in the sample don’t scintillate significantly, and those that do have been given special attention, we don’t believe that scintillation is strongly biasing our distribution. When we consider only the 31 not strongly scintillating, isolated pulsars above our luminosity cutoff, we find a best-fit slope of -0.86 ± 0.08 , consistent with that derived from all our isolated sample pulsars. We note further that since the known MSPs in the plane have mostly very low DMs ($\sim 80\%$ have $DM < 50 \text{ pc cm}^{-3}$) and are observed for shorter amounts of time (which means less averaging over strong scintillation epochs), scintillation is potentially a larger pitfall in analyzing the luminosities of those sources.

As the flux densities used in this analysis were obtained at either 0.43 GHz, 1.4 GHz, or 2.0 GHz (see Table 6) we have also investigated the uncertainty introduced by the error on the mean spectral index used to scale these fluxes. The nominal error on the -1.8 mean spectral index we have used is 0.2 (Maron et al. 2000). We have re-run our fitting of isolated

pulsars using a spectral index of -1.6 and -2.0 and find slopes of -0.92 ± 0.07 and -0.89 ± 0.07 respectively for isolated pulsars. Thus, uncertainty in the average spectral index of these pulsars does not have a large effect on the derived luminosity distribution.

Lastly, we have statistically compared the luminosity distributions of isolated and binary GC pulsars, using a Kolmogorov-Smirnov (KS) test (e.g. Press et al. 1986). We find that the two populations are statistically different with only 34% confidence. In other words, there is currently no evidence that the observed luminosity distributions of isolated and binary GC pulsars are significantly different. This can also be seen by plotting the best-fit slope from the distribution of isolated GC pulsars over the distribution of binaries (dashed-line in Figure 5, top right). This lack of difference has also been recently demonstrated for the MSPs in the Galactic plane by Lorimer et al. (2007), who argue that previous claims (Bailes et al. 1997; Lommen et al. 2006) of a statistical difference between the luminosities of the two populations were due to small number statistics and observational biases.

6. Conclusions

We have used the Arecibo radio telescope at ~ 1.4 GHz to search 22 GCs for pulsars. These searches are among the deepest searches ever undertaken for such objects, and employed the most sensitive algorithms available to find Doppler-shifted binary pulsar signals. Our survey discovered 11 MSPs, almost doubling the known population in these GCs. 8 of these new pulsars are in binary systems, and 3 show eclipses. We find a significantly higher proportion of binaries, eclipsing systems, and pulsars with very short spin periods ($P_{\text{spin}} < 4$ ms) than previous searches of these clusters. We consider the luminosity distribution of GC pulsars and find that these follow a form $d \log_{10}(N) = -0.90 \pm 0.07 d \log_{10}(L)$. We find no evidence for a difference in the luminosity distributions of isolated and binary GC pulsars.

J.W.T.H. thanks NSERC for a PGS-D fellowship, which was tenured during this research. I.H.S. holds an NSERC UFA and is supported by an NSERC Discovery Grant. V.M.K. is a Canada Research Chair, and acknowledges support from an NSERC Discovery Grant and Steacie Supplement, CIAR, and from the FQRNT. We sincerely acknowledge Arun Venkataraman, Jeff Hagen, and Bill Sisk of the Arecibo Observatory for their fantastic help with data management and maintenance of the WAPPs. We also thank Dunc Lorimer for his valuable guidance in our early days of WAPP use and Fernando Camilo, our referee, who provided detailed comments and suggestions which improved our original manuscript. V.M.K., J.W.T.H., and S.M.R. are very grateful to the Canada Foundation for Innovation

for the New Opportunities Grant that funded construction of “The Borg”, the computer cluster that was essential for our analysis, and to Paul Mercure for helping to maintain this system. The Arecibo Observatory is part of the National Astronomy and Ionosphere Center, which is operated by Cornell University under a cooperative agreement with the National Science Foundation.

REFERENCES

- Alpar, M. A., Cheng, A. F., Ruderman, M. A., & Shaham, J. 1982, *Nature*, 300, 728
- Anderson, S. B. 1993, Ph.D. Thesis, Caltech
- Anderson, S. B., Gorham, P. W., Kulkarni, S. R., Prince, T. A., & Wolszczan, A. 1990, *Nature*, 346, 42
- Bailes, M., Johnston, S., Bell, J. F., Lorimer, D. R., Stappers, B. W., Manchester, R. N., Lyne, A. G., Nicastro, L., D’Amico, N., & Gaensler, B. M. 1997, *ApJ*, 481, 386
- Bégin, S. 2006, M.Sc. Thesis, UBC
- Bhat, N. D. R., Cordes, J. M., Camilo, F., Nice, D. J., & Lorimer, D. R. 2004, *ApJ*, 605, 759
- Camilo, F., Lorimer, D. R., Freire, P., Lyne, A. G., & Manchester, R. N. 2000, *ApJ*, 535, 975
- Camilo, F. & Rasio, F. A. 2005, in *Astronomical Society of the Pacific Conference Series*, Vol. 328, *Binary Radio Pulsars*, ed. F. A. Rasio & I. H. Stairs, 147
- Chakrabarty, D., Morgan, E. H., Muno, M. P., Galloway, D. K., Wijnands, R., van der Klis, M., & Markwardt, C. B. 2003, *Nature*, 424, 42
- Chandler, A. M. 2003, Ph.D. Thesis, Caltech
- Cohn, H. N., Lugger, P. M., Grindlay, J. E., & Edmonds, P. D. 2002, *ApJ*, 571, 818
- Cordes, J. M. & Chernoff, D. F. 1997, *ApJ*, 482, 971
- Cordes, J. M. & Lazio, T. J. W. 2002, (astro-ph/0207156)
- D’Amico, N., Possenti, A., Fici, L., Manchester, R. N., Lyne, A. G., Camilo, F., & Sarkissian, J. 2002, *ApJ*, 570, L89

- D’Amico, N., Possenti, A., Manchester, R. N., Sarkissian, J., Lyne, A. G., & Camilo, F. 2001, *ApJ*, 561, L89
- Dewey, R. J., Taylor, J. H., Weisberg, J. M., & Stokes, G. H. 1985, *ApJ*, 294, L25
- Dotani, T., Asai, K., & Greiner, J. 1999, *PASJ*, 51, 519
- Dowd, A., Sisk, W., & Hagen, J. 2000, in *ASP Conf. Ser. 202: IAU Colloq. 177: Pulsar Astronomy - 2000 and Beyond*, 275
- Freire, P. C., Gupta, Y., Ransom, S. M., & Ishwara-Chandra, C. H. 2004, *ApJL*, 606, L53
- Freire, P. C., Kramer, M., Lyne, A. G., Camilo, F., Manchester, R. N., & D’Amico, N. 2001, *ApJ*, 557, L105
- Freire, P. C. C. 2005, in *ASP Conf. Ser. 328: Binary Radio Pulsars*, ed. F. A. Rasio & I. H. Stairs, 405
- Freire, P. C. C., Hessels, J. W. T., Nice, D. J., Ransom, S. M., Lorimer, D. R., & Stairs, I. H. 2005, *ApJ*, 621, 959
- Harris, W. E. 1996, *AJ*, 112, 1487
- Hessels, J. W. T., Ransom, S. M., Stairs, I. H., Freire, P. C. C., Kaspi, V. M., & Camilo, F. 2006, *Science*, 311, 1901
- Hut, P., McMillan, S., Goodman, J., Mateo, M., Phinney, E. S., Pryor, C., Richer, H. B., Verbunt, F., & Weinberg, M. 1992, *PASP*, 104, 981
- Johnston, H. M. & Kulkarni, S. R. 1991, *ApJ*, 368, 504
- Jouteux, S., Ramachandran, R., Stappers, B. W., Jonker, P. G., & van der Klis, M. 2002, *A&A*, 384, 532
- Kaplan, D. L., Escoffier, R. P., Lacasse, R. J., O’Neil, K., Ford, J. M., Ransom, S. M., Anderson, S. B., Cordes, J. M., Lazio, T. J. W., & Kulkarni, S. R. 2005, *PASP*, 117, 643
- Kramer, M., Xilouris, K. M., Lorimer, D. R., Doroshenko, O., Jessner, A., Wielebinski, R., Wolszczan, A., & Camilo, F. 1998, *ApJ*, 501, 270
- Kulkarni, S., Goss, W., Wolszczan, A., & Middleditch, J. 1990, *ApJ*, 363, L5
- Kulkarni, S. R., Anderson, S. B., Prince, T. A., & Wolszczan, A. 1991, *Nature*, 349, 47

- Lommen, A. N., Kipphorn, R. A., Nice, D. J., Splaver, E. M., Stairs, I. H., & Backer, D. C. 2006, *ApJ*, 642, 1012
- Lorimer, D. R., Faulkner, A. J., Lyne, A. G., Manchester, R. N., Kramer, M., McLaughlin, M. A., Hobbs, G., Possenti, A., Stairs, I. H., Camilo, F., Burgay, M., D’Amico, N., Corongiu, A., & Crawford, F. 2006, *MNRAS*, 372, 777
- Lorimer, D. R. & Kramer, M. 2004, *Handbook of Pulsar Astronomy* (Cambridge observing handbooks for research astronomers, Vol. 4. Cambridge, UK: Cambridge University Press, 2004)
- Lorimer, D. R., McLaughlin, M. A., Champion, D. J., & Stairs, I. H. 2007, *astro-ph/0705.0685*
- Lyne, A. G., Biggs, J. D., Brinklow, A., Ashworth, M., & McKenna, J. 1988, *Nature*, 332, 45
- Lyne, A. G., Biggs, J. D., Harrison, P. A., & Bailes, M. 1993, *Nature*, 361, 47
- Lyne, A. G., Johnston, S., Manchester, R. N., Staveley-Smith, L., & D’Amico, N. 1990, *Nature*, 347, 650
- Lyne, A. G., Manchester, R. N., Lorimer, D. R., Bailes, M., D’Amico, N., Tauris, T. M., Johnston, S., Bell, J. F., & Nicastro, L. 1998, *MNRAS*, 295, 743
- Lyne, A. G., Manchester, R. N., & Taylor, J. H. 1985, *MNRAS*, 213, 613
- Maron, O., Kijak, J., Kramer, M., & Wielebinski, R. 2000, *A&AS*, 147, 195
- McConnell, D., Deshpande, A. A., Connors, T., & Ables, J. G. 2004, *MNRAS*, 348, 1409
- Middleditch, J. & Kristian, J. 1984, *ApJ*, 279, 157
- Mott, A. J. & Freire, P. C. 2003, in *Bulletin of the American Astronomical Society*, 1292
- Ortolani, S., Barbuy, B., Bica, E., Zoccali, M., & Renzini, A. 2007, (*astro-ph/0705.4030*)
- Phinney, E. S. 1992, *Philos. Trans. Roy. Soc. London A*, 341, 39
- Possenti, A., D’Amico, N., Manchester, R. N., Camilo, F., Lyne, A. G., Sarkissian, J., & Corongiu, A. 2003, *ApJ*, 599, 475
- Press, W. H., Flannery, B. P., & Teukolsky, S. A. 1986, *Numerical Recipes. The Art of Scientific Computing* (Cambridge: University Press, 1986)

- Radhakrishnan, V. & Srinivasan, G. 1982, *Curr. Sci.*, 51, 1096
- Ransom, S. M., Cordes, J. M., & Eikenberry, S. S. 2003, *ApJ*, 589, 911
- Ransom, S. M., Eikenberry, S. S., & Middleditch, J. 2002, *AJ*, 124, 1788
- Ransom, S. M., Hessels, J. W. T., Stairs, I. H., Freire, P. C. C., Camilo, F., Kaspi, V. M., & Kaplan, D. L. 2005a, *Science*, 307, 892
- Ransom, S. M., Hessels, J. W. T., Stairs, I. H., Freire, P. C. C., Kaspi, V. M., & Camilo, F. 2005b, *American Astronomical Society Meeting Abstracts*, 207
- Ransom, S. M., Hessels, J. W. T., Stairs, I. H., Kaspi, V. M., Freire, P. C. C., & Backer, D. C. 2005c, in *ASP Conf. Ser. 328: Binary Radio Pulsars*, ed. F. A. Rasio & I. H. Stairs, 199
- Ransom, S. M., Stairs, I. H., Backer, D. C., Greenhill, L. J., Bassa, C. G., Hessels, J. W. T., & Kaspi, V. M. 2004, *ApJ*, 604, 328
- Sigurdsson, S. & Phinney, E. S. 1993, *ApJ*, 415, 631
- Sigurdsson, S. & Thorsett, S. E. 2005, in *ASP Conf. Ser. 328: Binary Radio Pulsars*, ed. F. A. Rasio & I. H. Stairs, 213
- Sipior, M. S., Portegies Zwart, S., & Nelemans, G. 2004, *MNRAS*, 354, L49
- Standish, E. M. 1998, *Interoffice Memo. 312.F-98-048*. Pasadena: JPL
- Tavani, M. 1991, *Nature*, 351, 39
- Thorsett, S. E., Arzoumanian, Z., Camilo, F., & Lyne, A. G. 1999, *ApJ*, 523, 763
- Toscano, M., Bailes, M., Manchester, R., & Sandhu, J. 1998, *ApJ*, 506, 863
- Wolszczan, A., Anderson, S., Kulkarni, S., & Prince, T. 1989a, *IAU Circ.*, 4880, 1
- Wolszczan, A., Kulkarni, S. R., Middleditch, J., Backer, D. C., Fruchter, A. S., & Dewey, R. J. 1989b, *Nature*, 337, 531
- Zoccali, M., Renzini, A., Ortolani, S., Bragaglia, A., Bohlin, R., Carretta, E., Ferraro, F. R., Gilmozzi, R., Holberg, J. B., Marconi, G., Rich, R. M., & Wesemael, F. 2001, *ApJ*, 553, 733

Table 1. Survey Source List and Observations

Catalog ID	Other Name	Distance (kpc)	r_c^a (arcmin)	ρ_o^b ($\log_{10} L_\odot/\text{pc}^3$)	Concentration ^c ($\log_{10} r_t/r_c$)	DM(Δ DM) ^d (pc cm^{-3})	Predicted DM ^d (pc cm^{-3})	Time Visible ^e (hrs)	Isolated ^f Pulsars	Binary ^f Pulsars	Lum. Limit ^g (mJy kpc^2)
NGC 4147*	...	19	0.10	3.48	1.80	...	24	2.8	6.8
NGC 5024*	M53	18	0.36	3.05	1.78	24	25	2.8	...	1	6.1
NGC 5053	...	16	1.98	0.53	0.84	...	25	2.7	5.0
NGC 5272*	M3	10	0.55	3.51	1.84	26.4(0.3)	23	2.5	...	4(4)	2.1
NGC 5466	...	16	1.64	0.88	1.32	...	22	2.4	5.7
NGC 5904*	M5	7.5	0.42	3.91	1.83	29.5(0.8)	32	1.5	1	4(3)	1.4
NGC 6205*	M13	7.7	0.78	3.33	1.51	30.2(1.1)	38	1.2	2(1)	3(2)	1.7
NGC 6426*	...	21	0.26	2.35	1.70	...	121	1.7	11
NGC 6535*	...	6.8	0.42	2.69	1.30	...	172	0.8	1.9
NGC 6749	Be42	7.9	0.77	3.33	0.83	193(2)	438	1.5	...	2(2)	2.0
NGC 6760*	...	7.4	0.33	3.84	1.59	200(6)	257	1.3	1	1	2.0
NGC 6779	M56	10	0.37	3.26	1.37	...	163	2.3	2.5
NGC 6838	M71	4.0	0.63	3.04	1.15	117	86	2.8	...	1(1)	0.3
NGC 6934*	...	16	0.25	3.43	1.53	...	83	2.2	6.6
NGC 7006*	...	42	0.24	2.46	1.42	...	74	2.7	34
NGC 7078*	M15	10	0.07	5.38	2.50	66.9(2.2)	68	2.6	7	1	2.1
NGC 7089	M2	12	0.34	3.90	1.80	...	46	0.6	5.3
Pal 2	...	28	0.24	3.76	1.45	...	136	2.3	18
Pal 5	...	23	3.25	-0.81	0.70	...	34	0.9	17
Pal 10	...	5.9	0.81	3.50	0.58	...	166	2.8	0.8
Pal 13	...	26	0.65	0.40	0.68	...	38	2.6	14
Pal 15	...	45	1.25	-0.27	0.60	...	77	0.7	76

Note. — Clusters marked with an asterisk (*) were also searched by Anderson (1993) with Arecibo at 430 MHz. Anderson (1993) also searched NGC 6218 (M12, no pulsars found), which is not visible using the Arecibo Gregorian dome. All previously known pulsars were found by Anderson (1993), with the exceptions of PSR J1911+0101B (Freire et al. 2005, in NGC 6760), PSRs B1516+02A and B (Wolszczan et al. 1989a, in M5), and PSR B2127+11A (Wolszczan et al. 1989b, in M15).

^aThe core radius of the cluster. For comparison, the half-power radius of the Arecibo 1.4-GHz beam is $\sim 1.5'$.

^bThe logarithm of the central luminosity density of the cluster.

^cThe logarithm of the ratio of the tidal radius to the core radius of the cluster.

^dPredicted values of DM are based on the Cordes & Lazio (2002) electron density model of the Galaxy. There is no formal uncertainty on these values, and the predicted DM can sometimes differ from the true value by a factor of two or more. The predicted DM is also provided for clusters with known pulsars, and this shows

the characteristic discrepancy between the values. In some cases, the predicted DM agrees very well with the DM of pulsars in the cluster. This is because these pulsars have been used to scale the model itself. For clusters with more than one known pulsar, ΔDM indicates the observed spread in DM.

^eTime visible with the Arecibo telescope, which can only track sources while they are within 20° of the zenith.

^fValues in parentheses indicate the number of pulsars in the cluster that were found in this survey. The numbers for NGC 5272 (M3) and NGC 6749 include one candidate pulsar (yet to be confirmed) each.

^gApproximate upper limit on the pseudo-luminosity at 1400 MHz ($L_{1400} = S_{1400}d^2$) of an undiscovered pulsar in the cluster. This assumes that the pulsar has a spin period $\gtrsim 1$ ms and is isolated.

Table 2. Comparison of Recent GC Pulsar Surveys

Telescope	Gain (K/Jy)	Bandwidth (MHz)	Int. Time (hr)	Obs. Freq. (GHz)
Arecibo	10.5	100	2	1.4
Parkes	0.7	288	8	1.4
GBT	2.0	600	8	2.0

Note. — Arecibo parameters are for the survey described here. Parkes parameters are for the Multibeam Filterbank system, used in a number of recent GC searches there (e.g. Camilo et al. 2000). GBT parameters are for surveys using the Pulsar Spigot (e.g. Ransom et al. 2005a).

Table 3. Previously Known Pulsars

Name Informal / Formal	Period (ms)	Isolated (I) or Binary (B)	Redetected? (Y/N)
M5A / PSR B1516+02A	5.554	I	Y
M5B / PSR B1516+02B	7.947	B	Y
M13A / PSR B1639+36A	10.378	I	Y
M13B / PSR B1639+36B	3.528	B	Y
M15A / PSR B2127+11A	110.665	I	Y
M15B / PSR B2127+11B	56.133	I	Y
M15C / PSR B2127+11C	30.529	B	Y
M15D / PSR B2127+11D	4.803	I	Y
M15E / PSR B2127+11E	4.651	I	Y
M15F / PSR B2127+11F	4.027	I	N ^a
M15G / PSR B2127+11G	37.660	I	N
M15H / PSR B2127+11H	6.743	I	N
M53A / B1310+18	33.163	B	Y
NGC 6760A / PSR B1908+00	3.619	B	Y
NGC 6760B / PSR J1911+0101B	5.384	I	Y

^aDetected in 327-MHz WAPP data, see §4.2.2.

Table 4. Pulsars and Their Basic Parameters

Name ^a Informal / Formal	Period (ms)	DM (pc cm ⁻³)	P_{orbit} (hr)	$a_1 \sin(i)/c$ (lt-s)	Min M_2 ^b (M_{\odot})	w_{50} ^c (%)	Flux Density ^d (μJy)	Number Det./Obs.	Span (MJD)
M3A / PSR J1342+2822A	2.545	26.5	Unk.	Unk.	Unk.	9.3	7	3/78	52491–52770
M3B / PSR J1342+2822B	2.389	26.2	34.0	1.88	0.21	8.2	14	16/78	52485–53335
M3C ^e / PSR J1342+2822C	2.166	26.5	Unk.	Unk.	Unk.	11	$\lesssim 6$	1/78	52337
M3D / PSR J1342+2822D	5.443	26.3	129 d	38.5	0.21	9.2	10	12/78	52768–53149
<i>M5A^f / PSR B1516+02A</i>	5.554	30.1	6.7	120		
<i>M5B / PSR B1516+02B</i>	7.947	29.5	165	3.05	0.11	20	25		
M5C ^g / PSR J1518+0204C	2.484	29.3	2.08	0.0573	0.038	6.2	39	59/60	52087–53422
M5D / PSR J1518+0204D	2.988	29.3	29.3	1.60	0.20	18	8	24/60	52090–53335
M5E / PSR J1518+0204E	3.182	29.3	26.3	1.15	0.15	7.9	10	12/60	52705–53399
<i>M13A^f / PSR B1639+36A</i>	10.378	30.4	11	140		
<i>M13B / PSR B1639+36B</i>	3.528	29.5	30.2	1.39	0.16	13	22		
M13C ^f / PSR J1641+3627C	3.722	30.1	5.5	30	60/67	52087–53422
M13D / PSR J1641+3627D	3.118	30.6	14.2	0.924	0.18	6.6	24	63/67	52087–53422
M13E ^g / PSR J1641+3627E	2.487	30.3	2.8 ± 0.2	0.037 ± 0.004	0.02	6.0	10	2/67	52892,52833
M71A ^g / PSR J1954+1847	4.888	117	4.24	0.0782	0.032	10	59	53/53	52082–53422
NGC 6749A / PSR J1905+0154A	3.193	194	19.5	0.588	0.090	16	23	17/17	52494–53
NGC 6749B ^e / PSR J1905+0154B	4.968	192	Unk.	Unk.	Unk.	7.8	$\lesssim 6$	1/17	52921

Note. — Unless otherwise indicated, errors on quantities are well below the level of the least significant figure quoted.

^aItalicized names are those of the previously known pulsars in clusters where new pulsars have been found.

^bAssuming a pulsar mass (M_1) of $1.4 M_{\odot}$ and orbital inclination $i = 90^{\circ}$.

^cFor profiles with multiple components, the width of the highest peak is given. As all the profiles suffer from residual dispersive smearing, these values represent upper limits on the intrinsic pulse width at this observing frequency.

^dFlux density at 1400 MHz. The approximate fractional uncertainty ranges from 30 – 70% depending on whether the source strongly scintillates and, if so, how often it was detected (see §5.3).

^eUnconfirmed candidate pulsar.

^fIsolated.

^gEclipses.

Table 5. Timing Solutions* for M3B, M3D, and NGC 6749A

	PSR J1342+2822B	PSR J1342+2822D	PSR J1905+0154A
Observation and data reduction parameters			
Period Epoch (MJD)	52770	52770	52770
Start time (MJD)	52763	52768	53070
End time (MJD)	53542	53476	54210
# of TOAs	161	83	77
TOA rms (μ s)	9.1	24	38
Timing parameters			
α^a	13 ^h 42 ^m 11 ^s .0871(1)	13 ^h 42 ^m 10 ^s .2(6)	19 ^h 05 ^m 15 ^s .4(4)
δ	+28°22′40″.141(2)	+28°22′36(14)″	+01°54′33(22)″
P (ms)	2.389420757786(1)	5.44297516(6)	3.19294082(1)
\dot{P}_{obs} (10^{-20})	1.858(4)	–	–
DM (cm^{-3} pc)	26.148(2)	26.34(2)	193.692(8)
P_b (days) ^b	1.417352298(2)	128.752(5)	0.81255243(2)
T_{asc} (MJD)	52485.9679712(6)	52655.38(4)	52493.83300(4)
x (s)	1.875655(2)	38.524(4)	0.58862(2)
e	–	0.0753(5)	–
Derived parameters			
θ_{\perp} (′)	0.14	0.23(12)	0.51(38)
\dot{P}_{int}	$< 3.4 \times 10^{-20}$	–	–
τ_c (Gyr)	> 1.1	–	–
B_0 (gauss)	$< 8.2 \times 10^7$	–	–
f (M_{\odot})	0.003526842(6)	0.0037031(8)	0.00033132(7)
m_c (M_{\odot}) ^c	0.21	0.21	0.090

*Note that the solutions presented for M3D and NGC 6749A are *not* completely phase-connected solutions. Due to sparse sampling, arbitrary phase jumps were used between some observing epochs (see §4.2.1).

^aThe uncertainties indicated for all parameters are twice the formal values given by TEMPO. We have used the Jet Propulsion Laboratory’s DE405 planetary ephemeris (Standish 1998) to derive these solutions.

^bThe orbital parameters are: orbital period (P_b), time of passage through the ascending node (T_{asc}), semi-major axis of the orbit of the pulsar, projected along the line-of-sight, divided by the speed of light (x) and orbital eccentricity (e). Since the latter quantity is too small to be measured, we can not estimate the longitude of the periastron relative to ascending node (ω). All other parameters are as described in the text.

^cTo calculate the minimum companion mass m_c , we assumed an inclination angle $i = 90^\circ$

and a pulsar mass of $1.4 M_{\odot}$.

Table 6. Sample of Pulsars Used for Luminosity Distribution

Cluster	Distance (kpc)	DM (pc cm ⁻³)	# Pulsars	Obs. Freq. (GHz)	Scintillating? (Y/N)
M5	7.5	29.5	5	1.4	Y
M13	7.7	30.2	5	1.4	Y
M15	10.3	66.9	8	0.4	N
M28	5.6	120.5	8	2.0	N
NGC 6440	8.4	223.4	5	2.0	N
NGC 6441	11.7	231.8	4	2.0	N
Terzan 5	8.7	238.0	33	1.4	N
47 Tuc	4.5	24.3	22	1.4	Y

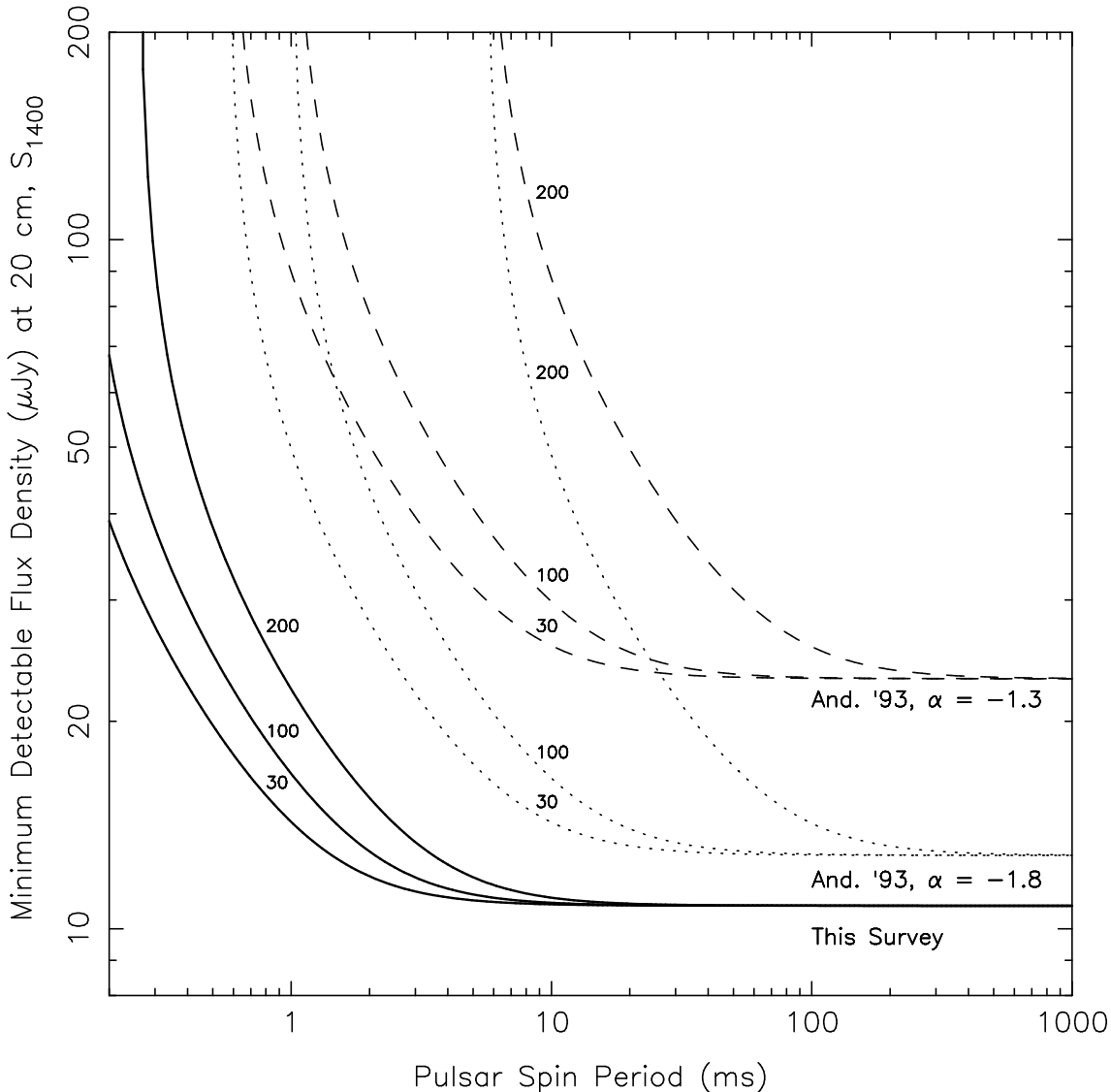


Fig. 1.— Survey sensitivity as a function of period and DM, assuming an intrinsic pulse width of 8% and an integration time of 2 hr. Each set of curves shows (from left to right) the sensitivity for DMs of 30, 100, and 200 pc cm^{-3} . The solid curves are the sensitivity of the survey described in this paper. The dotted (dashed) curves are the sensitivity of the 430 MHz survey of Anderson (1993) scaled to 1400 MHz assuming a spectral index of -1.8 (-1.3). For low-DM pulsars with periods $\gtrsim 10$ ms and steep spectral indices, the Anderson (1993) survey has comparable sensitivity. However, the survey presented here is significantly more sensitive to pulsars with periods $\lesssim 4$ ms, high DMs, and/or relatively flat spectral indices. The plotted survey sensitivity to slower pulsars ($P_{\text{spin}} \gtrsim 100$ ms) is likely significantly over-estimated by an unknown factor between 2 – 10 due to RFI and red noise (see §5.1.1).

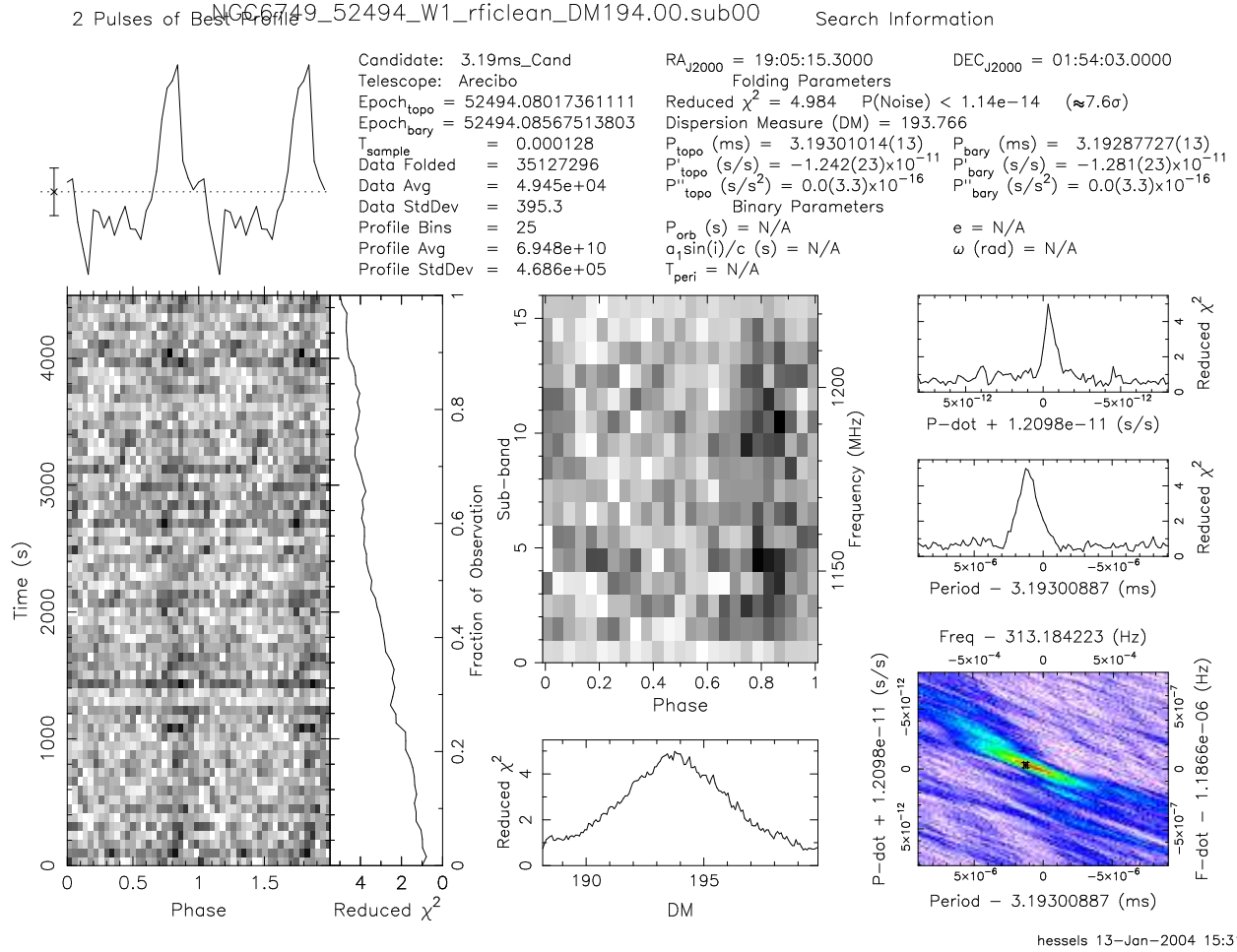


Fig. 2.— Sample candidate plot showing the various criteria on which a candidate is judged. The left-most panel shows the pulse intensity as a function of observing time and pulse phase (two cycles plotted) in greyscale, with the cumulative profile plotted at top and a side-bar at right showing the increase in the reduced χ^2 (measure of signal-to-noise ratio) with observing time. The top-middle greyscale panel shows the signal strength as a function of pulse phase and observing frequency (subband). The bottom-middle plot is the reduced χ^2 as a function of DM. The top-right (top-middle) panel shows the reduced χ^2 as a function of trial period derivative (period) at the best period (period derivative). Finally, the bottom-right panel shows the reduced χ^2 over a range of trial periods and period derivatives. During the folding, a range of DM, period, and period derivative are searched to produce the highest reduced χ^2 . This optimization improves on candidate parameters determined during the initial search. This is the discovery observation of NGC 6749A. The subbands show effects due to the masking of some of their constituent channels to remove RFI.

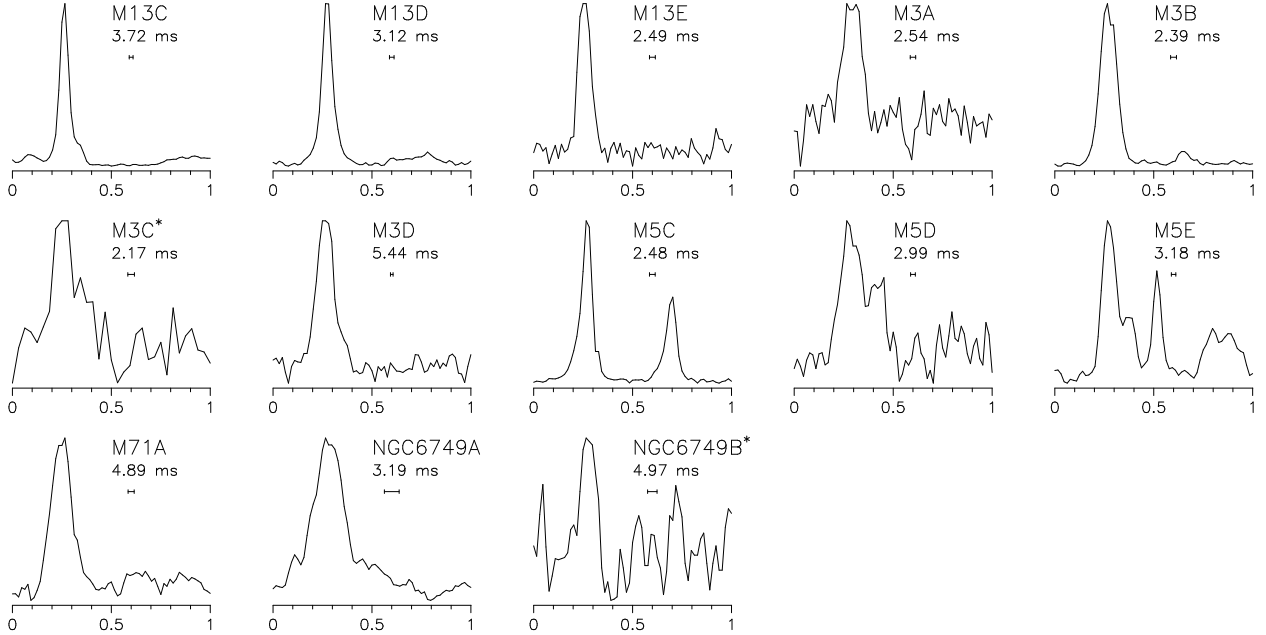


Fig. 3.— 1.4-GHz pulse profiles for the 11 millisecond pulsars and two promising candidates (marked with an asterisk) discovered in this survey. The profiles are often the sum of numerous observations and in the case of clusters where there is significant scintillation (i.e. M3, M5, and M13) the profiles are the sum of a few (or only one) observations where the pulsar appears much brighter than on average. The profiles have been rotated in phase so that pulse maximum occurs at 0.25. In each case, there are 64 bins across the profile, with the exception of M3C where 32 bins are used. The horizontal bar indicates the effective time resolution of the data, taking into consideration dispersive smearing. To aid the reader in interpreting what features in these profiles correspond to real emission, rather than spurious baseline fluctuations, we identify the following. M13C has low level emission preceding the main pulse and starting at phase 0.7. M13D may have a very weak interpulse around phase 0.75. M3B has a weak interpulse around phase 0.65. M5C has an interpulse around phase 0.7, which is of comparable strength to the main pulse. M5E has a duty cycle close to 100%, showing at least 3 significant peaks.

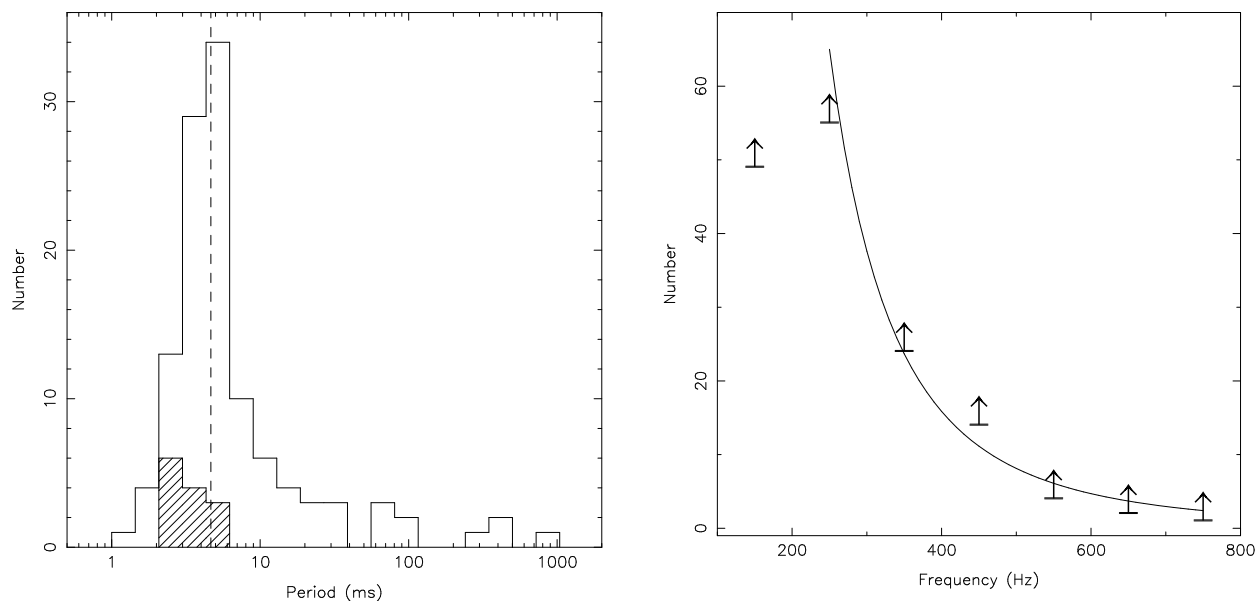


Fig. 4.— *Left:* Period histogram of 129 known GC pulsars (listed in <http://www.naic.edu/~pfreire/GCpsr.html>). The shaded area reflects pulsars found in the survey presented here. The vertical dashed line marks the median spin period of the observed population, 4.7 ms. *Right:* The combined population of MSPs in the field and GCs, plotted as a function of spin frequency. The points are binned in intervals of 100 Hz, and are shown as lower limits to reflect the various observational biases against detecting millisecond pulsars. The number of observed pulsars drops rapidly with spin frequency above 200 Hz, roughly as $N_{\text{psr}} \propto \nu_{\text{spin}}^{-3}$ (solid line).

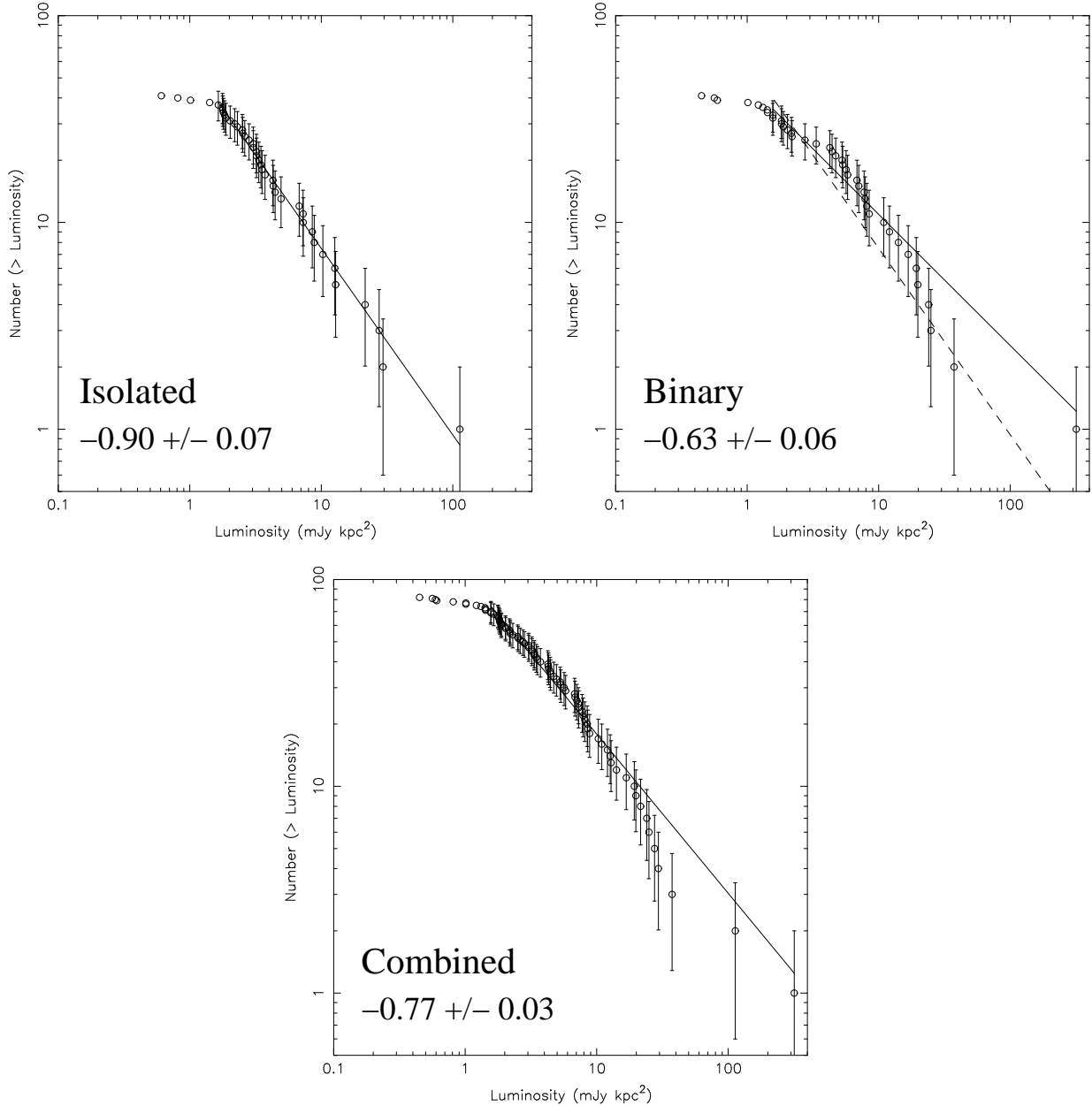


Fig. 5.— Cumulative distributions of 1.4-GHz luminosities of pulsars in M5, M13, M15, M28, NGC 6440, NGC 6441, 47 Tucanae, and Terzan 5. The minimum luminosity considered for fitting purposes is $L_{1400}^{\min} = 1.5 \text{ mJy kpc}^2$. Error bars are the square-root of each value. The excluded points below L_{1400}^{\min} are shown without error bars. *Top left:* luminosity distribution of 41 isolated pulsars in these clusters, which has a slope of -0.90 ± 0.07 (solid line, 37 pulsars used in fitting). *Top right:* luminosity distribution of 41 binary pulsars in these clusters, which has a slope of -0.63 ± 0.06 (solid line, 33 pulsars used in fitting). The best-fit slope from the distribution of isolated pulsars is also shown overlaid as a dashed line. *Bottom:* combined luminosity distribution, including all 82 isolated and binary pulsars. The best-fit slope is -0.77 ± 0.03 (solid line, 70 pulsars used in fitting).